BURNING RATE CHARACTERIZATION OF GUANIDINE NITRATE AND BASIC COPPER NITRATE PROPELLANTS WITH NANO- AND MICRON-SIZED METAL OXIDE ADDITIVES

A Thesis

by

ANDREW JOHN TYKOL

Submitted to the Office of Graduate and Professional Studies of
Texas A&M University
in partial fulfillment of the requirements for the degree of

MASTER OF SCIENCE

Chair of Committee,	Eric L. Petersen
Committee Members,	Waruna Kulatilaka
	Chad Mashuga
Head of Department,	Andreas A. Polycarpou

May 2018

Major Subject: Mechanical Engineering

ABSTRACT

Automotive airbag gas generants have been studied extensively to create formulations that meet both inflation and safety requirements. Additives have been used to increase the burning rates of these propellants, but the additive size has not been investigated. This thesis established the capability of studying such propellants at Texas A&M University for the first time and compared nano- and micron-sized additive burning rates and combustion characterization in guanidine nitrate (GN) and basic copper nitrate (BCN) composite propellants.

Three metal oxide additives were chosen for this study: aluminum oxide (Al_2O_3), ceria (CeO_2), and titania (TiO_2). They were tested in both their nano- and micron-sized forms at a mass loading of 4% to determine burning rate characterization differences. Formulations were mixed using a Resodyn acoustic mixer, and the samples were prepared using a hydraulic press. Resulting cylindrical pellets were then inhibited and burned over a range of pressures from 1000 psi (6.9 MPa) to 4000 psi (27.6 MPa).

Results from the burning rate experiments yielded in all formulations that the micron-sized additives performed better than their nano-sized counterparts. Also, all formulations except micron ceria performed worse than the stoichiometric GN/BCN baseline propellant. From the very different slag recovered from the burned propellants containing each additive, it was clear that the additives were affecting the propellant in different ways. It was concluded that due to the wide particle size range of the BCN used in this thesis, fewer catalytic reaction zones were being created for the nano-sized

particles, causing the additive to remove heat from the main GN/BCN reaction and ultimately inhibiting burning. The micron-sized additives removed heat to a lesser extent since they produced more catalyzed reaction zones when the small-sized BCN particles coated the additives. Future testing should focus on controlling the fuel and oxidizer size distribution to have more definitive results.

ACKNOWLEDGMENTS

I would like to thank my committee chair, Dr. Eric Petersen, for serving as my advisor throughout my time working in his research group. Serving as a research mentor as well as a teacher for multiple classes, he has taught me how to apply fundamental knowledge learned in the classroom to experimental research. I would also like to thank my fellow researchers and friends I have made while working in this research group: James Thomas, Catherine Dillier, Andrew Demko, and Erica Petersen. Additionally, I want to extend my appreciation to Dr. Waruna Kulatilaka and Dr. Chad Mashuga for serving on my committee. Lastly, I would like to thank my family for their continued support throughout my transition back to university and during my studies while here.

CONTRIBUTORS AND FUNDING SOURCES

This work was supported by a thesis committee consisting of Professors Eric Petersen and Waruna Kulatilaka of the Department of Mechanical Engineering and Professor Chad Mashuga of the Department of Chemical Engineering. Funding sources included an industry partner, Autoliv, which provided funding for the purchase of equipment and materials used during the tests in this thesis, and the Petersen Research Group. A LS 13 320 Laser Diffraction Particle Size Analyzer courtesy of Dr. Chad Mashuga's research group was used in this thesis. All work conducted for the thesis was completed by the student with the guidance of Dr. Eric Petersen.

NOMENCLATURE

a	Temperature coefficient
AN	Ammonium nitrate
AP	Ammonium perchlorate
AQ	Absolute quickness
BCN	Basic copper nitrate
CEA	Chemical equilibrium with applications
D_{Agg}	Agglomerate diameter
D_{AP}	AP diameter
DAQ	Data acquisition
DSC	Differential scanning calorimetry
f_c	Fractions of reactions catalyzed
FTIR	Fourier-transform infrared
GN	Guanidine nitrate
H_p	Enthalpy of the products
H_r	Enthalpy of the reactants
HRC	Rockwell hardness C
HTPB	Hydroxyl-terminated polybutadiene
JANAF	Joint army, navy, air force
l	Length
LD_{50}	Lethal dose that kills 50% of samples

MOPAC	Molecular orbital package
MS	Mass spectrometry
n	Pressure exponent or nano
P	Pressure
PDL	Pressure deflagration limit
r	Burning rate
RAM	Resonant acoustic mixing
SEM	Scanning electron microscope
σ_p	Temperature sensitivity at constant pressure
t	Time
T	Temperature
TGA	Thermogravimetric analysis
t_{GE}	Time to first gas evolution
t_{LE}	Time to first light emission

TABLE OF CONTENTS

Page

ABSTRACT ii

ACKNOWLEDGMENTS iv

CONTRIBUTORS AND FUNDING SOURCES v

NOMENCLATURE vi

TABLE OF CONTENTS viii

LIST OF FIGURES x

LIST OF TABLES xii

1. INTRODUCTION 1

1.1 Solid Propellants 1
1.2 Burning Rate Measurement 3
1.3 Automotive Airbag Operation 4
1.4 Objective and Outline 7

2. BACKGROUND 10

2.1 Automotive Airbag Propellant Requirements 10
2.2 Guanidine Nitrate and Basic Copper Nitrate Background 14
2.3 Fuel/Oxidizer Substitution Studies 20
2.4 Additive Studies 25
2.5 Propellant Preparation Methods 27
2.6 Particle Size 30

3. PROPELLANT FORMULATIONS 32

3.1 Propellant Formulations 32
3.2 Mixing Method 38

4. EXPERIMENTAL SETUP 43

4.1 Sample Preparation 43
4.2 Strand Burner and Data Acquisition 46

5. RESULTS AND DATA ANALYSIS 51

5.1 Material Properties 51
5.2 Burning Rates 53
5.3 Burning Rate Curves 55
5.4 Uncertainty Analysis 65

6. CONCLUSION AND RECOMMENDATIONS 67

REFERENCES 69

APPENDIX A 76

LIST OF FIGURES

Page

Figure 1 Typical airbag inflator unit found in a vehicle's steering wheel 6

Figure 2 Molecular structures of (a) GN and (b) BCN 15

Figure 3 GN/BCN TGA-DSC curves.....17

Figure 4 Four stages of GN/BCN/ Fe_2O_3 combustion reaction 19

Figure 5 Powders of sieved (a) GN and as-received (b) BCN 32

Figure 6 Laser diffraction particle size analyzer and BCN sample testing courtesy of Dr. Chad Mashuga's research group 33

Figure 7 GN particle size distribution.....34

Figure 8 BCN particle size distribution.....35

Figure 9 GN/BCN mixture particle size distribution 35

Figure 10 Acoustic mixing with large and micron-sized oscillating flow fields 40

Figure 11 Resodyn Mixer.....41

Figure 12 Propellant before (top) and after (bottom) mixing.....42

Figure 13 Computer generated pellet punch cutaway showing how a powdered propellant is pressed into a pellet.....43

Figure 14 Pellet punch components 44

Figure 15 Carver press 45

Figure 16 Pellet punch loaded between the platens of the press.....45

Figure 17 High-pressure, constant-volume testing vessel.....47

Figure 18 Bolt used to hold the propellant sample for testing 48

Figure 19 Pressed sample loading process.....48

Figure 20 Test facility experimental setup.....50

Figure 21 Burn time extracted from pressure and light trace 54

Figure 22 Aluminum oxide burning rate curves 57

Figure 23 Ceria burning rate curves 57

Figure 24 Titania burning rate curves 58

Figure 25 Typical slag recovered from (a) baseline, (b) aluminum oxide, (c) ceria, and (d) titania formulations 60

Figure 26 GN represented as red, BCN as blue, and additive as green 64

LIST OF TABLES

Page

Table 1 USCAR24 effluent gas limits....13
Table 2 GN/BCN mixture ratios....16
Table 3 Particle size analysis results....36
Table 4 Propellant formulations utilized in the present study....38
Table 5 Chemical properties used for theoretical calculations....51
Table 6 Density and adiabatic flame temperature of the tested formulations....52
Table 7 Combustion product properties....53
Table 8 Experimentally determined burning rates and pressure rise....55
Table 9 Experimentally determined burning rate equation variables....59

1. INTRODUCTION

1.1 Solid Propellants

Solid propellants play a vital role in several different industries. They are used for human-rated launch vehicles, missile propulsion, automotive airbag inflation, and much more. Their simplicity, low cost, reliability, and wide range of performance make them an ideal choice for many applications. These propellants consist of a premixed fuel and oxidizer that remains unreacted until there is a source of ignition. Once a typical solid propellant is ignited, it will burn to completion creating high temperature and pressure gases used for either propulsive or gas generative purposes. Solid propellants are classified into two categories: double-base propellants and composite propellants. Double-base propellants create a highly energetic, homogeneous mixture of fuel and oxidizer. They usually consist of sold nitrocellulose which absorbs liquid nitroglycerine, both of which are a fuel and oxidizer themselves [1]. Composite propellants form a heterogeneous mixture of fuel and oxidizer that are either held together by an oven-cured binder and curing agent or compacted into a pellet. Often, composite propellants are modified with metals and metal oxide additives which act as a catalyst, tailoring the propellant's performance for specific applications. Additives allow a propellant to have an increased or decreased burning rate as well as a plateau effect. In many applications, a plateau effect is particularly advantageous, allowing a propellant to burn consistently regardless of pressure variations.

The automotive industry utilizes solid composite propellants for gas generation in airbag applications. These propellants are not used for thrust, thus it is desired to have a low combustion temperature and high, non-toxic gas output. Early airbags relied on alkali metal azide-based propellants, predominantly sodium azide (NaN_3). Sodium azide was popular due to its reasonable gas output, low reaction temperatures, and non-toxic combustion products (pure nitrogen gas), but there are numerous disadvantages to this propellant as well [2]. Prior to combustion, sodium azide is highly toxic, having an LD_{50} of 45 mg/kg, requiring special handling for manufacture as well as end of useful life disposal [3]. There are several cases in which factory workers have had minor to major health problems after working with the compound. This chemical is also hazardous if it undergoes hydrolysis, producing highly toxic and potentially explosive hydrazoic acid (HN_3). This very unstable gas can form explosive solids upon reacting with heavy metals such as copper, so great care must be taken to eliminate any possibility of water or moisture interactions [4]. With the many exceedingly dangerous properties of sodium azide, there has been a push to find superior gas generant propellants that still meet the required gas output and toxicity requirements.

There has been research into new propellant formulations containing chemicals such as guanidine nitrate (GN), 5-aminotetrazole (AT), nitroguanidine (NQ), guanylurea nitrate, or triaminoguanidine azide (TAGZ) that act as the propellant fuel; and basic copper nitrate (BCN), ammonium perchlorate (AP), ammonium nitrate (AN), sodium nitrate, potassium nitrate, or potassium perchlorate that serve as the oxidizer [3,5–13]. These fuels and oxidizers have been mixed in several combinations to meet strict criteria

for being a suitable airbag inflator propellant which requires adequate burning rate and gas output, low toxicity, and low gas exhaust temperature. The above list is not all encompassing but rather just a snapshot of the many fuel and oxidizer combinations that have been studied over the past twenty years. From this list, a very common gas generant used in today's airbags is composed of guanidine nitrate (GN) and basic copper nitrate (BCN). This propellant serves as the standard to which many of the other developmental propellants are compared. GN/BCN is the current standard for many reasons. Acting as the fuel, GN is relatively inexpensive, readily available, and also contains oxygen itself, helping reduce the amount of oxidizer required for reaction. Serving as the oxidizer, BCN is also relatively inexpensive, readily available, has a high gas output, and has good thermal stability [8,14–17]. GN/BCN is the selected propellant for this study because of its many advantageous properties and its widespread acceptance.

1.2 Burning Rate Measurement

Unlike liquid propellants, solid propellants cannot be throttled to control their burning rate. A typical solid propellant will burn to completion once ignited, and to characterize its performance the propellant is first tested in a small-scale strand burner. It is very important to characterize a propellant's burning rate to determine its performance in varying environmental and combustion chamber conditions where temperatures and pressures can reach extreme values. When conducting a burning rate experiment in a strand burner, a typical output will be a curve that plots pressure transducer voltage and time. There is then a calibration step which converts the pressure transducer output

voltage into pressure. The pressure versus time curve can then be used to back out several important performance parameters such as burn time and pressure rise. Additional data can be collected from this setup using a light emission sensor. This sensor captures light intensity, with an output in voltage, and can be plotted against the burn time as well. Using the pressure curve, light trace curve, and also a high-speed camera, the time of the burn can be extracted reliably and accurately. Once the time of the burn is experimentally determined, the burning rate can be found using Equation 1.

$$r = \frac{l}{\Delta t} \quad \textbf{(1)}$$

In this equation, the initial sample length, l, and the burn time, Δt, are used to determine the linear burning rate, r.

1.3 Automotive Airbag Operation

The automotive airbag is a passive restraint safety device that complements the seatbelt for high-impact collisions. It consists of many components that work together simultaneously to inflate an airbag in a fraction of a second after a collision to protect the automobile occupant. There are three main components: a collision sensor, an inflator assembly, and an airbag. First, the collision sensor is a continually sensing device that is used to determine if there has been a collision. It is very sensitive since it first must determine if the crash is significant enough to deploy the airbags and second, the location of the impact and which airbags it must signal to initiate ignition. All of this assessment must be done in about 20 to 25 milliseconds and is called the sensing time [18]. The collision sensor also ensures that the airbag does not deploy during low-speed

collisions as this could injure the occupant more than the collision itself, assuming a seat belt is worn. With this safety requirement in mind, there has been a generally accept threshold limit for low-speed airbag deployment. In order to protect both occupants who wear and don't wear seat belts, an airbag will generally deploy if the frontal crash sensor measures an impact of 12 mph or greater. This lower limit is not a set value and varies for different cars, having a grey area from 8 to 14 mph where an airbag never deploys below 8 mph and always deploys above 14 mph [18]. If there is a collision at a speed high enough to trigger the crash sensor, then the sensor will send a signal to ignite the gas-generating propellant in the inflator assembly.

There are two main types of inflator assemblies: a pyrotechnic gas generator and a hybrid gas generator, which utilizes pyrotechnics as well as compressed gas. A hybrid gas generator will have a small amount of pyrotechnic material that will initially ignite once a collision occurs. Once ignited, the pyrotechnics will rupture a membrane on the compressed gas chamber allowing the gas, such as nitrogen, to fill the airbag. This hybrid generator is advantageous since there is only a small amount of pyrotechnics, allowing for very low inflator gas toxicity as well as low gas temperatures [19]. The main disadvantage for the hybrid system is the size and weight of the compressed gas tank, many times being too large to fit into the steering wheel. On the other hand, pyrotechnic gas systems are quite compact and lightweight. The inflator assembly is concentric, allowing for easy storage in a steering wheel, and it has three main compartments, each with a specific purpose. Figure 1 shows a typical inflator unit [19].

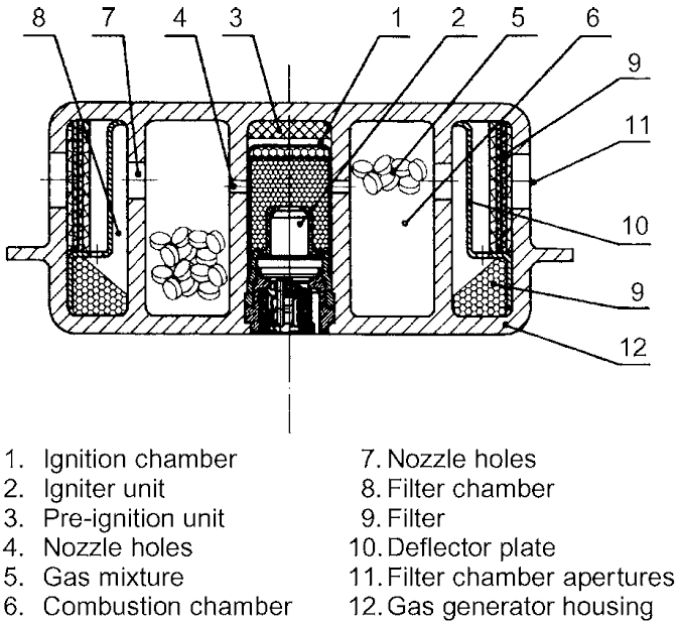

Figure 1 Typical airbag inflator unit found in a vehicle's steering wheel. Reprinted from [19]

The first and central chambers are where the initiator or igniter is housed, usually containing 0.02 g to 0.03 g of igniter material per gram of gas generant [18]. The pyrotechnic squib in this chamber is usually a boron/potassium nitrate mixture that releases high temperature and pressure gases once ignited by an electric current [2,4]. These combustion products flow through orifices into the combustion chamber, igniting the primary gas generant. This generant is typically in the form of compressed pellets, in the amount of about 75 to 100 grams for the driver's inflator, and upon combustion releases gas to inflate the airbag as well as some liquid/solid residual byproducts which must be filtered out [18]. Both the igniter and combustion chamber are designed for pressures up to 60 MPa, with the igniter chamber working pressures are around 100 to 180 bar [2,19]. The generant gas then flows into the lower-pressure filter chamber which

consists of several screens, baffles, and wire mesh devices used to filter and cool the gas and liquid/solid slag before exiting concentric orifices into the airbag [4,18]. The ignition chamber, combustion chamber, and primary filter are hermetically sealed in an aluminum container, allowing for a long shelf life and propellant ignition reliability [4]. The airbag is the final component of this safety system which is inflated with the combustion gases and unfolds through slotted plastic panels. A typical airbag is about 60 liters in volume and upon inflation will have an internal pressure of about 6 psig [18]. Once ignition occurs, the airbag is fully inflated within 30 milliseconds [18,19]. If sensing time and inflation time are combined, from the instant of a collision to full deployment of the airbag, it is only about 55 milliseconds. This extremely fast response is of the upmost importance since barrier crash test studies have shown that at only 35 mph an unrestrained occupant's head would impact the windshield in about 76 milliseconds [18].

1.4 Objective and Outline

Guanidine nitrate and basic copper nitrate propellant meet most of the inflator's requirements, but there is still room for improvement. GN/BCN suffers from a lower than desired burning rate making the propellant unsuitable for applications such as side airbag deployment, which requires airbag inflation in even less time than the frontal airbags [13,16]. With this limitation in mind, the burning rate can be increased in a couple different ways. First, part of the fuel (GN) or oxidizer (BCN) can be substituted with a component that burns at a higher rate. This tradeoff has been studied with many

different fuel and oxidizer mixtures with the aim to create a reliable and safe propellant, some of which are listed in Section 1.1. Second, additives can be used to increase the burning rate. Metal oxides are the most common additives, acting as catalysts, and they can have significant effects, with loadings normally below 5% by weight. Performance increases have been seen in guanidine-based propellants and also AP/HTPB propellants, which are commonly used in the Petersen Research Group. In a guanidine-based study, increasing the concentration of copper (II) oxide from 0% to 5% by weight increased the burning rate by 33% [20]. Furthermore, past research has shown that additive size can have significant effects on the burning characteristics of AP/HTPB propellants [21]. This size effect however is not always true as observed in previous projects from the Petersen Research Group in which nanoparticles actually slightly reduced burning rate compared to micron-sized particles in AP/HTPB propellants [22]. Lund and Bradford [23] have shown in guanidine-based propellants that nano-sized silicon dioxide and aluminum oxide performed worse than other micron-sized additives, but direct comparison of additive size to itself has not been researched for common airbag propellant formulations. The purpose of this thesis was to characterize the ballistic properties of a commonly used airbag gas-generating propellant (guanidine nitrate and basic copper nitrate) with nano- and micron-sized metal oxide additives. This was done by comparing the burning rate of aluminum oxide (Al_2O_3), ceria (CeO_2), and titania (TiO_2) in their nano- and micron-sized forms. A Resodyn resonant acoustic mixer (RAM), which utilizes low-frequency and high-intensity acoustic energy, was used to mix each formulation.

The following sections in this thesis first provide a background of important automotive airbag gas generant properties followed by past studies conducted with GN and/or BCN as well as other fuels and oxidizers. Next, GN/BCN propellant formulations and mixing methods are laid out and explained. Experimental setup and procedures follow, describing the experimental test setup and the preparation of samples. The data collection and analysis section shows results, and an uncertainty analysis was performed and its results are presented. With all experimental information analyzed, conclusions are made and recommendations for future work are laid out.

2. BACKGROUND

2.1 Automotive Airbag Propellant Requirements

Airbags are in all modern automotive vehicles, and as technology progresses the standard for airbag safety becomes higher. Airbags and the gas-generant propellants they utilize must adhere to these strict standards and support the absolute best technology to protect the public. With the life of vehicles extending, airbags must be reliable for the entire life of the vehicle, in many cases for ten or more years.

There are many key requirements for an airbag propellant. First and foremost, as mentioned in Section 1.3, an airbag must be fully deployed in about 25 - 30 milliseconds. For this rapid deployment to occur, the gas generant must ignite and burn to completion, releasing combustion product gases into the bag. This expulsion of gas requires an adequate propellant burning rate, usually 0.4 - 0.5 inches per second and more preferably 1.0 - 1.2 inches per second at 1000 psi [3,5]. Performance must not be significantly degraded when the gas generant is burned at extreme environmental conditions. It is desired that the propellant have a low temperature sensitivity, which can be expressed by Equation 2 [1].

$$\sigma_p = \left(\frac{\delta ln r}{\delta T}\right)_p \quad \textbf{(2)}$$

Temperature sensitivity, σ_p, is expressed by the change in burning rate per degree change in propellant temperature at constant pressure. Adequately low temperature sensitivity for airbag propellants is less than 0.002 K^{-1} [10]. This value means that the propellant will burn at an acceptable rate to fill the airbag in the required time even at low

temperature where burning rates usually decrease. Propellant pressure sensitivity should also be low, with an exponent value of 0.35 or more desirably 0.30, allowing the propellant to burn consistently without large burning rate fluctuations due to changing chamber pressures [20].

It is also important that the temperature of combustion stay relatively low so the combustion gases do not burn the vehicle occupant when deployed. It is generally desired that these flame temperatures stay below 2200 to 2300 K [13,24]. The filters, while sieving out any solid or liquid residue, also help reduce the gas temperature before entering the airbag, acting as heat sinks. Solid and liquid residues are desired to be less than 10 - 12 grams per mole of gas produced [8]. Furthermore, as stated in Section 1.3, a typical driver side airbag is about 60 liters in volume and contains 75 - 100 grams of propellant. There is a range in the propellant amount because some release more gas per mole than others and they must release enough gaseous products adequately fill the airbag. Additionally, in Lund and Bradford's [23] patent, they state that a suitable propellant density lies between 1.8 and 2.2 g/cc. Barnes and Taylor [24] state that a propellant must produce greater than 2 moles per 100 grams of generant to be effective. Other than being highly toxic, another reason why there has been a move away from sodium azide is because it does not produce ample amounts of gaseous products, releasing only about 0.30 - 0.35 liters of gas per gram of generant [19]. On the other hand, many of the organic fuel compounds, such as guanidine nitrate, are nitrogen rich and can release up to 0.50 - 0.65 liters of gas per gram of generant [19]. The desired propellant properties listed above mostly deal with performance, but as mentioned

before, airbags must remain reliable for over ten years, so propellant stability is of upmost importance as well.

An airbag propellant must be thermally stable, and common industry practice states that propellants should remain stable when aged at 107 °C for over 400 hours and also maintain structural stability when cycled between -40 °C and 107 °C [5]. This temperature requirement is very practical since environmental conditions can easily reach those extreme temperatures in certain parts of the world. If the propellant were to decompose inside of the testing range, the passenger would be at risk of an airbag that would possibly not inflate as intended. Yamato [8] conducted a similar thermal stability experiment in which he placed several propellant formulations in a constant-temperature bath, at 105 °C, for 400 hours. These propellants were mostly unaffected, with most showing less than 0.15% weight loss. Additionally, practice states that a propellant should not decompose at temperature below 160 °C and should not readily absorb moisture [13,25]. It has been seen that propellant moisture content below 0.2% can be advantageous against aging and can also lead to pressure exponent reduction [26]. Lastly, with performance and stability requirements for a propellant covered, toxicity must be low and handling must be easy for a propellant to be viable.

A viable propellant must be safe to handle during manufacture and end-of-life disposal and also release large amounts of non-toxic gas, in many cases nitrogen. Sodium azide was once the standard as it produced a reasonable amount of gas, but mainly because its gaseous combustion products were all non-toxic nitrogen as seen in Equation 3.

$$2NaN_3 \rightarrow 2Na + 3N_2 \quad \textbf{(3)}$$

Although all nitrogen gas products are highly desirable, as mentioned in Section 1.1, sodium azide is highly toxic when unreacted. This toxicity is unacceptable since it has led to manufacture and disposal worker health problems. With this potential hazard in mind, many current propellants are organic, have lower toxicity, and contain carbon, hydrogen, nitrogen, and oxygen. For example, guanidine nitrate has an LD_{50} of 730 mg/kg, a moderate-to-low toxicity [27]. Having a lower toxicity is advantageous, but this relative safety comes at a price since most organic propellants contain additional elements that can lead to toxic gaseous combustion products. Table 1 shows some airbag effluent gas limits that have been put in place by the United States Council for Automotive Research [28]. An organic propellant is more likely to meet these

Table 1 USCAR24 effluent gas limits. Adapted from [28]

Effluent Gas	Vehicle Level Limit (ppm)	Driver-Side Limit (ppm)
Chlorine (Cl_2)	1	0.25
Carbon monoxide (CO)	461	115
Carbon dioxide (CO_2)	30000	7500
Phosgene ($COCl_2$)	0.33	0.08
Nitric oxide (NO)	75	18.75
Nitrogen dioxide (NO_2)	5	1.25
Ammonia (NH_3)	35	9
Hydrogen chloride (HCl)	5	1.25
Sulphor dioxide (SO_2)	5	1.25
Hydrogen sulfide (H_2S)	15	3.75
Benzene (C_6H_6)	22.5	5.63
Hydrogen cyanide (HCN)	4.7	1.18
Formaldehyde (HCHO)	1	0.25

requirements if it has an oxygen balance (OB) near 0%, in the range of +/- 5% [20]. This oxygen balance is at or near the stoichiometric ratio of fuel to oxidizer and allows for full combustion to occur, limiting the amount of toxic gases released.

It is clear that there are many regulations and industry practices that ensure airbag propellants work as intended. These regulations are essential and promote the safety of the vehicle occupant as well as the workers that handle the propellant during manufacture and disposal.

2.2 Guanidine Nitrate and Basic Copper Nitrate Background

Guanidine nitrate is a water-soluble salt and fuel that acts partially as an oxidizer as well since it contains oxygen. Its chemical formula is $CH_6N_4O_3$, and it contains about 46% nitrogen by weight allowing it to produce large amounts of nitrogen gas upon combustion. GN has many advantageous properties including low impact sensitivity (50 N·m with no reaction), low friction sensitivity (353 N, no reaction), and has a moderately high decomposition temperature of 270 °C [2]. It has a -26.2% oxygen balance, so an oxidizer in needed for increased burning rate and complete combustion to occur. Basic copper nitrate, $Cu(NO_3)_2 \cdot 3Cu(OH)_2$, is an oxidizer with high gas output and good thermal stability. Figure 2 shows both chemical structures. When burned as a

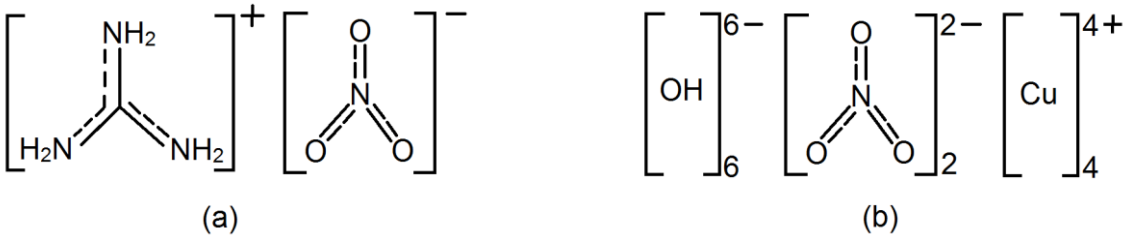

Figure 2 Molecular structures of (a) GN and (b) BCN

single composite propellant at a stoichiometric ratio, it produces a high gas yield with relatively low effluents. Equation 4 shows the balanced stoichiometric reaction between GN and BCN.

$$9CH_6N_4O_3 + 2[Cu(NO_3)_2 \cdot 3Cu(OH)_2] \rightarrow 9CO_2 + 33H_2O + 20N_2 + 8Cu \quad \textbf{(4)}$$

Stoichiometric, fuel rich, fuel lean, and additive thermal decomposition studies have been conducted on this formulation, determining the mechanisms of decomposition between the two compounds.

Mei et al. [15] conducted a study on the thermal decomposition of GN/BCN. The ratio of GN/BCN was varied from 100% GN to 100% BCN. The mass ratio of GN/BCN of 62.24/37.76 resulted in the largest heat of reaction, releasing 3152.7 J/g of heat. This correlates to a -5 oxygen balance. This result is within the desired +/- 5% OB range to reduce effluents from partial combustion [20]. As the oxygen balance becomes positive, excess BCN absorbs additional heat, lowering the heat of reaction. The pure GN sample decomposes endothermically. The first peak occurs at about 213 ºC, which represents the GN melting. At about 278 ºC, GN enters its main decomposition stage, losing 72.8% of its mass by the time it reaches 320 ºC. Nakashima et al. [14] found very similar results for pure GN samples with endothermic peaks at 213 ºC and 302 ºC, which again aligns

with the GN melting point of 215 ºC and thermal decomposition starting at 270 ºC [2]. Furthermore, Damse [12] suggests that the slow decomposition rate is due to the slow breakage of relatively strong C-N bonds. These bonds cannot be homolytically cleaved like N-NH_2 bonds found in triaminoguanidine azide (TAGAZ), which was found to decompose at a faster rate. It was concluded that two C-NH_2 amino group bonds were broken, forming a GN weight fraction of 74.4%, which aligns with the decomposition mass loss of about 75%. This sequence leads to the slower-than-desired burning rate of pure GN. The pure BCN sample only had one peak, which was endothermic and starts decomposition at about 219 ºC. Similar results were found in more recent literature, with BCN decomposition at 215 ºC [14]. The final mass loss was 34% which indicates that the solid residue is mainly copper oxide (CuO), which represents about 66.25% by mass of the BCN. Table 2 shows the mixture ratios studied, and Figure 3 shows the respective mixtures thermogravimetric analysis (TGA) and differential scanning calorimetry (DSC) curves [15]. It was determined that decomposition of GN/BCN mixtures occurred in three phases: dissociation and escape of crystal water, solid GN/solid BCN phase reaction, and liquid GN/solid BCN phase reaction.

Table 2 GN/BCN mixture ratios. Adapted from [15]

#	GN/BCN		Oxygen
	Mol Ratio	Mass Ratio	Balance (%)
1	100/0	100/0	-26
2	90.90/9.10	71.14/28.86	-10
3	86.64/13.36	62.24/37.76	-5
4	81.82/18.18	53.35/46.65	0
5	75.90/24.10	44.46/55.54	5
6	68.47/31.53	35.57/64.43	10
7	0/100	0/100	30

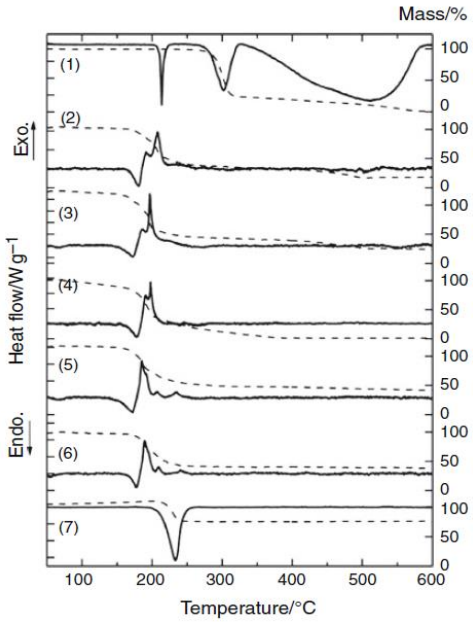

Figure 3 GN/BCN TGA-DSC curves. Reprinted from [15]

The TGA-DSC curves showed that during the first phase, there is an endothermic peak between 170-180 °C where crystal water dissociates. The second peak is exothermic at 185 °C, which is below the onset melting temperature of GN (198 °C) and the onset decomposition temperature of BCN (204 °C). This feature is the solid-solid phase reaction just before the GN melts. The third peak is exothermic at about 200 °C and represents the onset of melted GN increasing contact area with the BCN, releasing the largest amount of heat. It can be seen that as the amount of GN decreases, the third peak also decreases since there is less melted GN to come into contact with BCN, thus increasing the second solid-solid phase reaction peak. Additionally, gas product analysis of the -5 OB sample was performed using TGA/DSC along with mass spectrometry (MS) and Fourier-transform infrared (FTIR) spectroscopy. MS found possible species N, O or NH_2, OH or NH_3, H_2O, CO or N_2, NO, and CO_2 or N_2O. FTIR spectroscopy found

H_2O, N_2O, and CO_2 in the products. Comparing MS and FTIR, it can be concluded that H_2O, N_2, N_2O, and CO_2 exist with nearly no NO or CO.

Nakashima et al. [14] conducted a thermal decomposition and gas analysis study on a stoichiometric GN/BCN formulation. The thermal decomposition results aligned with the Mei et al. [15] study. Additionally, evolved gas analysis indicated that pure GN had FTIR spectroscopy peaks for CO_2, N_2O, NO_2, and NH_3. Oxley et al. [29] proposed several possible decomposition routes for GN, some of which are the evolved gas products found by Nakashima et al. [14]. GN can decompose by dissociation to nitric acid (HNO_3) and ammonia (NH_3). Nitric acid can further decompose into water and nitrogen dioxide (NO_2). Another pathway is via dehydration, where nitroguanidine and water are products. It is also possible that ammonium nitrate (NH_4NO_3) is an intermediate in GN decomposition, which then decomposes further to nitrous oxide (N_2O) and water. Pure BCN had a peak for NO_2, and GN/BCN had peaks for H_2O, N_2O, and CO_2. The GN/BCN FTIR results align with previous research [15]. Since N_2O was common to both pure substances but not the mixture, there may be some neutralizing reaction with H_2O. FTIR spectroscopy of GN/BCN combustion gases revealed that only CO_2 and H_2O were generated. Equilibrium calculations discovered that the decomposition temperature of N_2O was below the adiabatic flame temperature of GN/BCN, thus why it is not present after combustion. Furthermore, it was demonstrated that NO_x tends to decrease with increasing pressure, but CO and NH_3 remain the same. This result could be explained by the fact that high pressures directly increase the burning rate, thus having a shorter residence time for the oxidation of N_2 to occur and NO_x to form.

Mei et al. [7] conducted another GB/BCN thermal decomposition study in which part of the BCN was substituted with iron oxide (Fe_2O_3) that had an average particle size of 5.02 microns. The supplement of this additive reduces the heat of combustion, combustion rate, and flame temperature. The GN/ BCN/Fe_2O_3 reaction occurs in four stages: pre-heat, condensation, combustion, and cooling. Figure 4 shows the stages of this combustion reaction [7]. Pre-heat starts as the grains are heated until the GN melts at 215 °C. After melting, condensation quickly ensues until combustion occurs at a slower rate. The final stage take place as the combustion residue cools.

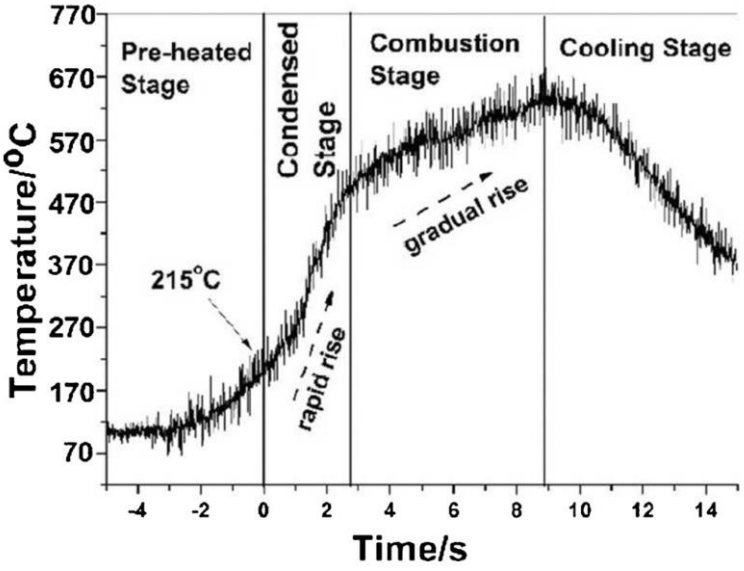

Figure 4 Four stages of GN/BCN/ Fe_2O_3 combustion reaction. Reprinted from [7]

The onset reaction of GN/ Fe_2O_3 takes place at 257.9 °C, which is higher than the temperature at the end of the GN/ BCN/Fe_2O_3 reaction, about 250 °C. From this information, it can be concluded that the iron oxide reacts mainly with BCN in the GN/BCN mixture, possibly with Cu or CuO that is formed during combustion. The additive mixture showed similar TGA-DSC curves as the GN/BCN formulation, indicating that

similar reaction processes are occurring. Another noteworthy finding is that mixtures containing iron oxide had reaction onset temperatures about 50 °C higher than GN/BCN formulations, indicating that iron oxide increases the thermal stability of the propellant. Furthermore, the addition of iron oxide decreased the burning rate of the propellant.

2.3 Fuel/Oxidizer Substitution Studies

GN/BCN is the current standard for gas generant airbag propellants, but there is always room for improvements in terms of burning rate enhancement, combustion temperature reduction, and pressure exponent reduction, etc. There are numerous studies in which GN or BCN are either fully or partially substituted with another promising fuel or oxidizer. These studies propose some promising formulations, although it is not always clear whether the new formulations are superior. In many cases when one performance parameter is increased, another decreases. Cost, availability, and ease of manufacturability are also concerns that must be taken into account.

Seo et al. [9] conducted a study in which the fuel and additives were kept constant, varying the mass percentage and size of the oxidizers. Guanidine nitrate was the fuel component with a mixture of basic cupper nitrate, ammonium perchlorate, and sodium nitrate as oxidizers. The characterization technique absolute quickness (AQ) was used to determine the slope of the pressure versus time experimental output from 25% to 75% of the maximum pressure. Essentially, this number relates to the burning rate of a propellant, with higher values correlating with higher burning rates. It was found that increasing the amount of ammonium perchlorate from 8% by weight to 13% increases

the maximum pressure by about 9%. Additionally, when the size of basic copper nitrate was decreased from 44 microns to 22 microns the AQ increased by about 46%. Both maximum pressure and AQ, or burning rate, are important performance parameters for proper airbag operation. A smaller-sized BCN particle will lead to increased burning rate and faster airbag deployment.

Engelen and Lefebvre [6] inspected several different fuel and oxidizer combinations for combustion gas properties. GN combined with potassium nitrate (KNO_3) or potassium perchlorate ($KClO_4$) was included in this study. A closed bomb experimental setup with a gaseous igniting mixture (CH_4/O_2) was used to burn the cylindrical samples. Ignition was not successful for pure GN or GN/KNO_3 at 0.18 MPa, but ignition was successful for GN/$KClO_4$ at 0.28 MPa. This formulation resulted in 130 ppm NO, 1 ppm NO_2, <20 ppm CH_4 (due to gaseous ignition fuel), <20 NH_3, and <5 HCN. All of these effluent concentrations except NO meet the United States Council for Automotive Research vehicle effluent requirements laid out previously in Table 1, section 2.1 [28]. Additionally, the GN/$KClO_4$ mixture produced about 1.43 moles/100g of gas, which is slightly below the desired 2 moles/100g [24]. Additionally, Engelen et al. [30] discovered that the GN/KNO_3 formulation had a 26 to 63 millisecond ignition delay time, a maximum pressure from 148 to 166 bar, and a time to maximum pressure of 227 to 256 milliseconds. These results were compiled after five tests were run. Furthermore, it was interesting that this specific formulation had burning rates that did not continually increase with pressure, as the other formulations did, but was more of a u-shaped pattern. These specific characteristics are not ideal for an airbag gas generant,

as one wants a shorter delay and a burning rate curve that is linear. With gas generation required in such a short amount of time, Ulas and Kuo [11] conducted a study on ignition delay time for several propellant formulations.

Most solid propellant combustion studies utilize a nichrome wire for ignition, and one study was found to use a gaseous ignition mixture, but laser ignition is viable also [6,14,31]. Ulas and Kuo [11] investigated the use of a CO_2 laser for ignition of several different solid propellants, one of which was a guanidine nitrate baseline. The baseline propellant contained (by weight) 31.3% GN, 54.2% ammonium nitrate (AN), 9.5% potassium nitrate, and 5% polyvinyl alcohol. Five other mixtures were tested: baseline with 0.1 - 0.2% carbon black; baseline with ammonium perchlorate (AP); baseline with RDX; baseline with triamino guanidine nitrate (TAGN); and baseline with RDX/TAGN. The last four mixtures contained 10 - 30% additive level in the correct amount to keep the oxygen balance constant. Tests were conducted in a constant-pressure, two-chamber vessel with a constant flow of either air or argon with pressures ranging from 1 to 69 atm. The laser intensity was also varied, with tests conducted at 30, 50, and 100 W/cm^2. Self-sustained burning and ignition delay time were the main focus of this study. It was determined that the baseline would only show self-sustained burning in 1-atm argon with laser power of 100 W/cm^2. Only the formulations that contained TAGN were able to maintain combustion at 1 atm after the 50 W/cm^2 laser was cut off. Higher heat fluxes were not tested for all formulations. Even though half of the formulations did not exhibit self-sustained burning, ignition delay time was still obtained for each one. Ignition delay time can be broken into two parts: time to first gas evolution

(t_{GE}) and time to first light emission (t_{LE}). t_{GE} is characterized by the inert heating of the propellant from the laser heat flux until gas evolves, which is a condensed-phase chemical process that is independent of pressure [32,33]. t_{LE} occurs once continuous heating causes the gases to experience pyrolysis, forming a visible reaction which is considered a flame [34]. For all samples, it was found that as laser heat flux increased, both ignition delay time parameters decreased. Furthermore, increasing the pressure generally reduces the $t_{LE,}$ but does not have much effect on t_{GE}. The baseline formulation and the RDX formulation had the shortest ignition delays, with t_{GE} delays for almost all formulations under 0.2 seconds. t_{LE} was mostly below 2 seconds, with a few around 30 seconds, and one at about 100 seconds. Having a short ignition delay time is one important parameter, but there are several more, a few of which include pressure sensitivity and temperature sensitivity.

A study characterizing ballistic properties such as pressure deflagration limit (PDL), burning rate, and temperature sensitivity of a guanidine based propellant was conducted by Ulas et al. [10]. The propellant formulation consisted of (by weight) 58.5% GN, 23.5% AP, 17.8% sodium nitrate, and 0.2% silicon dioxide. Temperature was varied from -30 to 100 °C and pressures ranged from 2.86 to 128 MPa. PDL results revealed that this limit is sensitive to propellant density with densities over 1.62 g/cc having a PDL of 7.34 to 8.03 MPa, and densities of 1.56-1.61 g/cc having a PDL of 8.37 to 8.72 MPa. Strand bomb burning experiments showed that this formulation produced highly reproducible burning rate curves. At lower pressures, below 17 MPa, burning was seen to be non-one-dimensional. A low-pressure dynamic melt layer made layer-by-layer

burning unachievable until the pressure was raised to about 20.8 MPa. Additionally, it was also discovered that a low temperature sensitivity of 0.001 - 0.002 K^{-1} was achievable. It was also observed that residual beads were formed and are thought to be mostly sodium chloride (NaCl). An optimal gas generant would have a low PDL and low temperature sensitivity to endure any environment it may encounter during its lifetime.

Guanylurea nitrate (fuel) and copper diamine dinitrate (oxidizer) were studied to determine if performance could be increased when substituting them into a GN/BCN propellant [13]. Performance parameters included gas yield (moles/100g), flame temperature (K), burning rate at 1000 psi (in/sec), and pressure exponent reduction. It was found that copper diamine dinitrate increases the gas yield, flame temperature, and pressure exponent but decreases the burning rate. Guanylurea nitrate increased the burning rate, reduced the flame temperature, and reduced the pressure exponent while maintaining a similar gas yield. From these results, guanylurea nitrate makes a very suitable substitute for guanidine nitrate in gas generant propellants. A lower pressure exponent helps reduce pressure dependence, while a lower combustion temperature improves effluents and also reduces the risk of burns for vehicle occupants. Copper diamine dinitrate raises the combustion temperature significantly and also decreases the burning rate, making it a less-than-ideal substitute for BCN. Mendenhall [25] furthered this study by creating a metal complex of guanylurea nitrate to be used as a fuel.

Copper II guanylurea dinitrate (CuGUN) is a copper complex of guanylurea nitrate whose burning rate characteristics were studied by Mendenhall [25]. This fuel was compared against the standard GN/BCN gas generant. Loading of CuGUN was

increased from 0 to 30% by weight in a GN/BCN/Al_2O_3 propellant formulation. A mass loading of 30% CuGUN was found to increase the burning rate by 32%, while increasing the pressure exponent moderately and having comparable gas yield. Flame temperature was also decreased by almost 250 K. In the right amount, CuGUN could be a promising fuel in combination with GN/BCN propellants. The formulation could be tailored to have an increased burning rate and lower flame temperature while also meeting pressure dependence requirements.

In another set of experiments, copper complexes of diammonium bitetrazole were added into a GN/BCN mixture. It was found that by adding these chemicals to the GN/BCN formulation it could increase the burning rate at 1000 psi by up to 44% [31]. Additionally, Wada et al. [35] investigated GN/BCN/AN mixtures and discovered that BCN was required for ignition and sustained combustion at low pressures. Increased AN loading led to lower pressure dependence of the propellant, with n about 0.41 - 0.45. Numerous more studies have been conducted, some containing the base GN/BCN formulation and others with different fuels, oxidizers, and additives, all of which were performed in hopes of finding the ideal airbag gas generant [3,5,8,16,20,23,24,36–48].

2.4 Additive Studies

Metal oxide burning rate enhancers were examined in GN/BCN formulations as well as GN/BCN formulations with Copper bis ethylenediamine dinitrate (CuEDDN), a fuel substitute [16]. Metal oxides tested include aluminum oxide (Al_2O_3), silicon dioxide (SiO_2), titania (TiO_2), zinc oxide (ZnO), magnesium oxide (MgO), and zirconium

dioxide (ZrO_2). First, GN/BCN/CuEDDN was examined by varying amounts of aluminum oxide and silicon dioxide from 1 to 5% by weight. Results show that silicon dioxide greatly increased solid slag recovery, which is desirable due to its easy filterability, but reduces burning rate as its amount is increased. Aluminum oxide increased slag recovery only moderately and increased burning rate for all loadings except 5%. To find a middle ground, silicon dioxide and aluminum oxide were loaded simultaneously into the formulation ranging from 1 to 4%. In all cases, burning rate was decreased, but slag recovery was greatly increased (100% recovery for all but one test). It is important to note that the burning rate with mixed oxides was still higher than the formulations that only contained silicon dioxide, so a mixture of silicon dioxide and aluminum oxide is advantageous since 100% recovery is possible with only moderately reduced burning rate.

The next sets of tests were conducted with the standard GN/BCN formulations, again with varied loadings of silicon dioxide and aluminum oxide. The standard GN/BCN formulation had a burning rate of 0.28 inches per second with liquid, amorphous slag. When silicon dioxide was added, up to 5%, the burning rate was very similar and slag became solid. When aluminum oxide was added at 2.5% loading, the burning rate increased by almost 100% and slag was solid, but soft. Again, the two metal oxides were mixed into the formulation, yielding an increased burning rate (25% increase) and solid slag. Though slag was all solid, more tests should be done if it is desired to have a higher burning rate since it is generally desired that the burning rate be at least 0.4 – 0.5 inches per second [3,5]. Lastly, additional metal oxides (all listed

previously) were tested at a 5% loading level and reviewed for burning rate enhancement as well as pressure exponent reduction in the base propellant GN/BCN/CuEDDN. All additives increased the pressure exponent, while burning rate was increased by only two, zinc oxide and magnesium oxide. More testing of these two additives, percent loading studies and slag recovery studies, could be done to determine if these are variable metal oxide additives.

2.5 Propellant Preparation Methods

Propellant formulations have been prepared in many ways, from their chemical synthesis to their forming process. These propellant formulations are usually all powder ingredients, which have been dry and wet blended to promote mixing. Dry mixing is the easiest and most basic method. In one study, powders were sieved through a 74-micron sieve three times to mix [7]. Wet mixing has also been done by dissolving GN in 50 ml of water heated to 90 °C. The remaining dry mixture (oxidizer and additives) was then added into the slurry and stirred. The slurry dried in a vacuum oven at 80 °C [31]. One of the most promising methods of mixing is slurry mixing followed by spray drying.

Lund and Bradford [23] state that their method of preparing a gas generant grain has up to a 20% increase in burning rate compared to other methods such as roll compacting, milling and/or mechanically mixing. The propellant on which they tested their method was GN/BCN/$KClO_4$. Spray dried powders are easier to handle and are more likely to press into uniform pellets without cracks or voids. Spray drying involves mixing the fuel into an aqueous slurry in which it is first dissolved. The oxidizer

particles are then added to the slurry and mixed. This slurry can then be sprayed through a nozzle via a stream of droplets that are heated by hot air which removes moisture from the particles. The resulting powder usually has a resulting size of about 100 to 200 microns. These are highly spherical particles, which have improved viscosity and are easy to handle and press into pellets.

Barnes and Smith [17] took the spray drying method one step further by investigated an improved method for producing spray dried propellants containing a basic metal nitrate. This new method was found to simplify and reduce the number of processing steps. The old method first reacted copper nitrate with sodium hydroxide in an aqueous solution to form BCN. The solution was then spry dried and combined with the fuel and additives in aqueous slurry which again was spray dried to form the final propellant powder. The newly proposed method simply combines all ingredients (copper nitrate, sodium hydroxide, GN, additives) at one time into a glass-jacketed reactor and once BCN was formed, it was spray dried to form the propellant powder. This new *in-situ* method was compared to the original method in which BCN was formed separately then mixed with GN/additives. It was discovered that the new method produced equivalent results to the old method, thus reducing processing steps and saving on costs. Additional reaction slurry mixtures and spray drying processes have been studied for other fuel/oxidizer combinations as well [37–39].

Once all of the ingredients are mixed in the desired manner, the powdered propellant now must be formed into a pellet. For this process, a hydraulic press is normally used, having a predefined program that runs for a specific time and force. An

automatic press is the most economical way to produce mass quantities of propellant due to high output and controllability [26,47]. In industry, it was found that powders are normally pressed at 12,000 pounds of force to 0.5 inches in diameter and about 0.5 inches in height [13,31]. Ulas et al. [10] were much more detailed with their pressing method, stating that powders were first dried to 90 °C to ensure any moisture present would be removed. The powder was then pressed to form cylindrical pellets with strict density requirements. Pressing included 138 MPa pressure held for a minute, then increased to 241 MPa for one minute, and lastly increased to 345 MPa for ten minutes. Density of 1.62 g/cc or greater were required. Pellets have also been modified after pressing, such as drilling holes through them, to be compatible with the laboratory's experimental setup [14]. In this particular setup, two wires were passed through the pellet (fuse-wire technique) to measure the distance and time the burn takes to pass both wires.

Once the pellet is formed, the next step is to coat one flat surface and its cylindrical surface with an inhibitor. This is done so that the pellet does not have an artificially increased burning rate due to side wall burning. The inhibitor allows the pellet to burn in a linear manner. This inhibitor has been seen to be a krylon spray paint as well as an epoxy resin [14,31]. Lastly, an ignitor powder is usually used to ensure good, reproducible pellet ignition. This powder is usually black powder, a boron and potassium nitrate mixture that is ignited via a nichrome wire [4,5,14,15,30,31,36].

2.6 Particle Size

Several different patents and journal articles have used different particle sizes for their fuel and oxidizer. Henry et al. [49] states that the particle size of guanidine nitrate is important and should be between 75 and 350 microns or more preferably 100 to 200 microns. The oxidizer particle size should be between 50 and 200 microns or more preferably 75 to 125 microns. Zeuner et al. [20] states that the fuel and oxidizer are desired to be less than 15 microns in size and preferably less than 10 microns. These smaller size particles help increase combustion rate for fast inflation actions such as belt tensioners. This finding is in agreement with Lundstorm and Shaw [4] who believe that particle sizes of gas generant materials are not particularly important unless one is trying to have very rapid combustion and in that case near sub-micron size of 0.7 to 0.9 microns is desirable. Furthermore, Seo et al. [9] discovered that as the size of BCN decreases, an increase in burning rate is observed. In journal articles, the size of GN has been seen ranging from 5.52 to 212 microns and BCN ranging from 1.63 to 44 microns [7,9,14,15]. Additionally, not only size but sphericity plays an important role in powder formation. Spray drying GB/BCN/$KClO_4$ leads to more uniformly rounded particles, sized at about 100 to 200 microns that are easier to handle and press [23]. Another important but less-studied parameter relates to the particle size of the additive.

Additive size studies are scarce, and the ones found in the literature did not directly compare nano- to micron-sized additives. Zeuner et al. [20] states that additives are desired to be less than 5 microns in size and preferably less than 1 micron. The patent states that these fine particles improve readiness to ignite and reduce ignition

delays, though it does not mention anything quantitatively. In another patent, Lund and Bradford [23] express that silicon dioxide is preferred in a nano-size of about 7 to 20 nanometers, but can be up to 50 nanometers. Silicon dioxide helps produce glassy, solid slag that can be easily filtered and improves the viscosity of the powder mixture. It is implied that this additive reduces the burning rate due to its sub-micron size and that another, larger additive can be used to increase the burning rate, but as seen by Mendenhall et al. [16], silicon dioxide already reduces burning rate. So, it is unclear whether silicon dioxide is reducing the burning rate even further due to its nano-size. In the same study, it was found that other micron-sized metal oxide additives increased the burning rate more than nano-sized silicon dioxide and aluminum oxide. Silicon dioxide and aluminum oxide were not tested in their micron-sized form, so it cannot be concluded if their performance was lower due to their size.

3. PROPELLANT FORMULATIONS

3.1 Propellant Formulations

Guanidine nitrate and basic copper nitrate were the fuel and oxidizer on which this study was focused. Equation 4 in section 2.2 shows the stoichiometric equation for GN/BCN complete combustion. Complete combustion will limit effluents and provide the maximum amount of non-toxic gases. The reactant molar ratio in this equation will be used. This proportion corresponds to a GN/BCN molar ratio of 81.82:18.18 and a mass ratio of 53.36:46.64. These two ingredients are in a powdered form as seen in Figure 5. GN powder was purchased from Sigma-Aldrich, but particle size was not

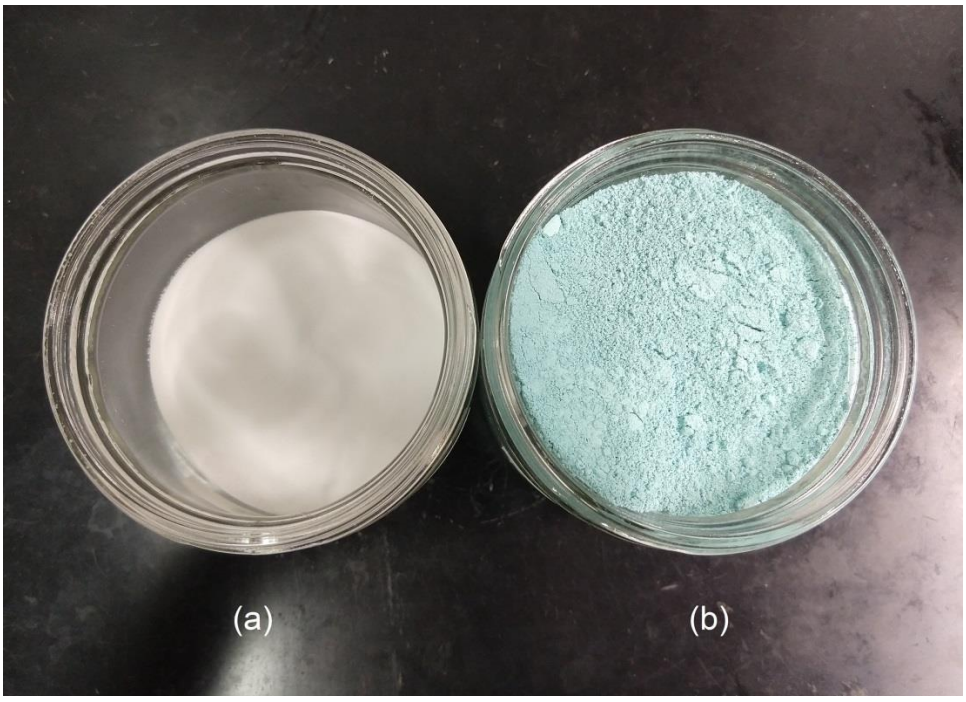

Figure 5 Powders of sieved (a) GN and as-received (b) BCN

mentioned. The powder was sieved through several mesh sizes, and it was found that there was a wide range of particle sizes. The powder selected passed through the 212-µm sieve and remained on top of the 180-µm sieve mesh. BCN was purchased from Pyro Chem Source. This powder did not sieve easily due to agglomerations, but particle sizing was provided by the manufacturer, so sieving was omitted. Additional in-house particle sizing analysis was performed using a laser diffraction particle size analyzer as seen in Figure 6. This analysis is based on the Fraunhofer diffraction theory, which states that

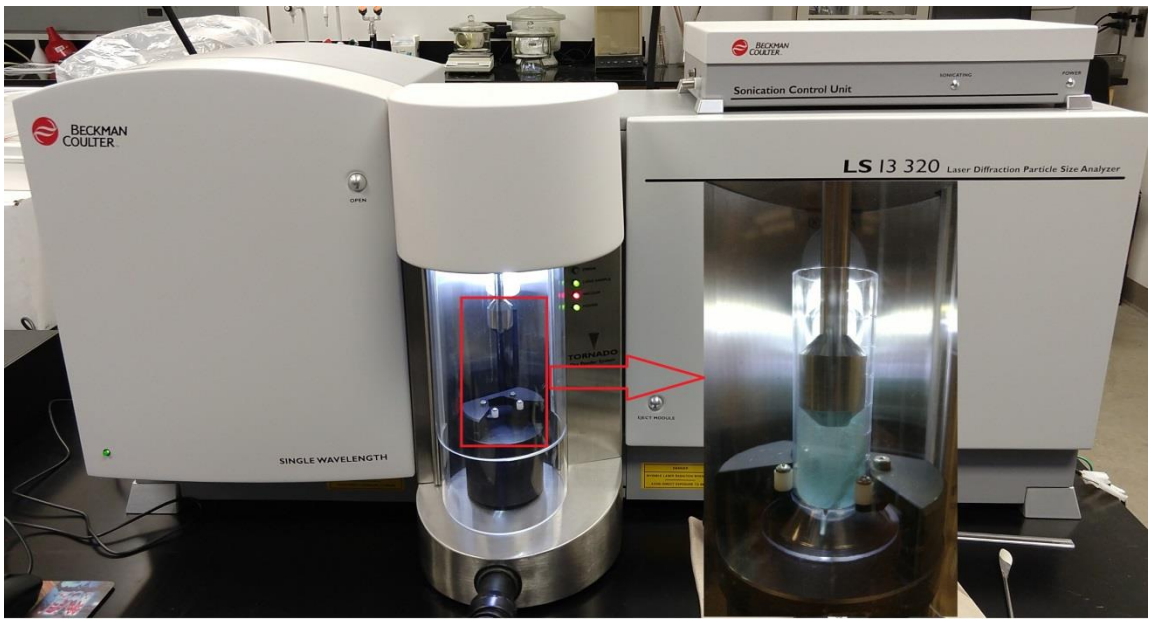

Figure 6 Laser diffraction particle size analyzer and BCN sample testing courtesy of Dr. Chad Mashuga's research group

the size of a particle affects the angle in which light is diffracted; as the particle size decreases, the angle of diffracted light increases. Fraunhofer diffraction is only practical for particle sizes greater than 0.5 µm because any smaller diameter approaches the wavelength of light and the theory is no longer valid [50]. Particle sizing results for GN,

BCN, and the GN/BCN mixture can be seen in Figure 7, Figure 8, and Figure 9, respectively. It is evident that the particles have a wide range, with BCN varying the most. Graph statistics are summarized in Table 3.

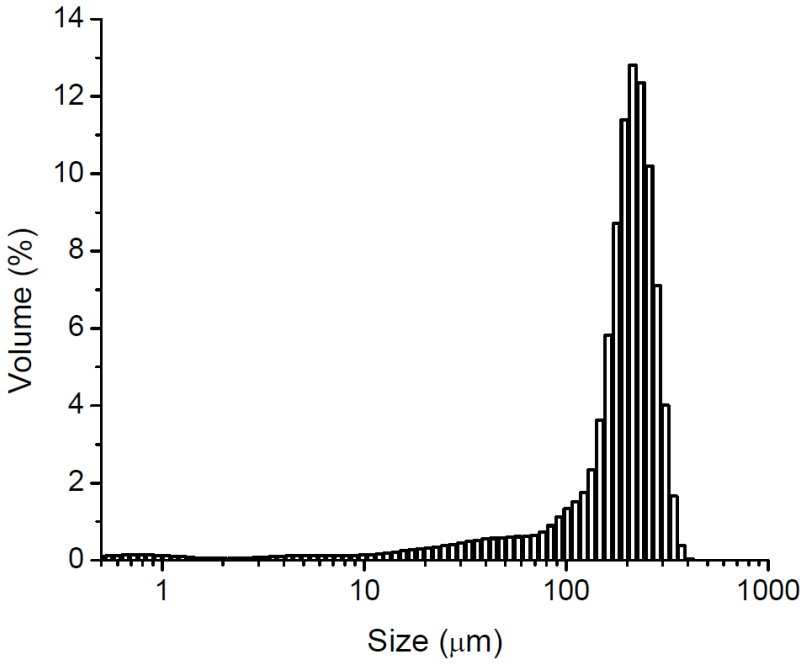

Figure 7 GN particle size distribution

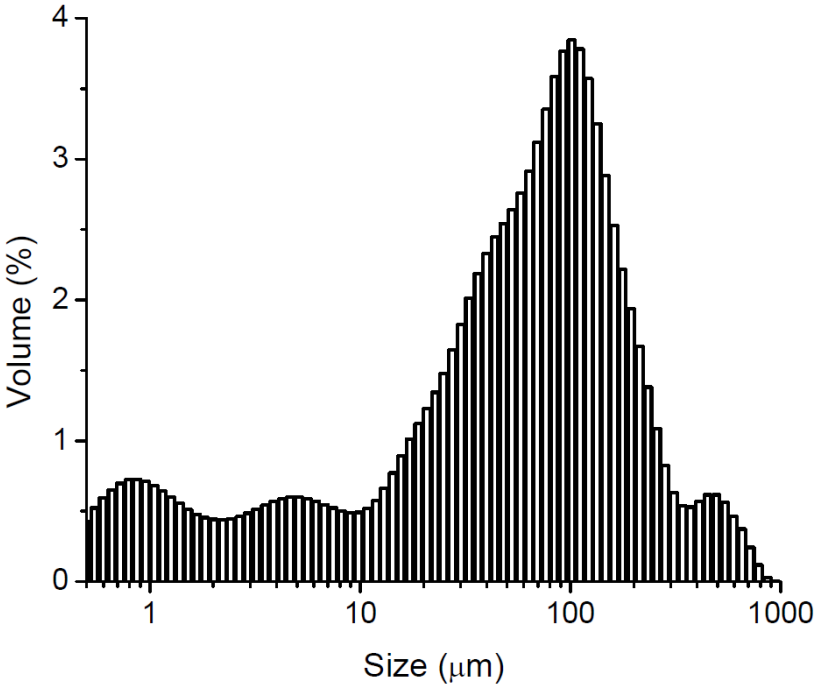

Figure 8 BCN particle size distribution

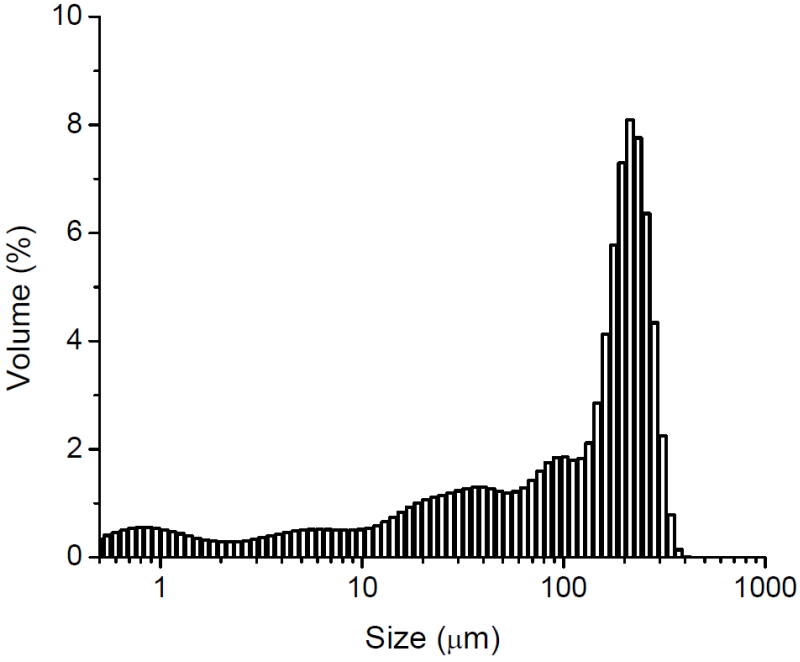

Figure 9 GN/BCN mixture particle size distribution

Table 3 Particle size analysis results

Chemical	Average Particle Size (μm)	D10 (μm)	D50 (μm)	D90 (μm)
GN	197.40	55.09	210.80	294.40
BCN	98.33	2.19	65.58	216.50
BCN*	-	0.93	2.59	10.82
GN/BCN	137.40	4.36	145.50	272.30

*Manufacturer provided BCN sizing data

Statistics include average particle size as well as D10, D50, and D90 which represent the percent of the sample by mass which is comprised of particles smaller than the specified size. For example, D50 of 210.80 μm represents that 50% (by mass) of the particles in the mixture are less than 210.80 μm. It is important to note that the manufacturer of BCN stated distribution values much lower than the present analysis results. It is hard to conclude true particle size without further analysis, such as scanning electron microscope (SEM) imaging. From the information available, a few conclusions can be made. Figure 7 shows that GN particle size has its largest peak at about 200 μm with a long, but fairly low-volume tail. On the other hand, Figure 8 shows BCN particle sizing has several large peaks, with the largest around 100 μm. BCN's tail volume is much larger on both sides of the main peak, extending all the way to 1000 μm. A comparison can be made to Figure 9, the GN/BCN mixture. This distribution shows that there are no particles sized over 400 μm. This is interesting since BCN had a peak at 500 μm and particles as large as 1000 μm. This leads to a conclusion that when mixed, some of the "larger particles" in the BCN sample were actually agglomerations that broke up during mixing. When handling the BCN powder, it was evident that it was very fine and agglomerations were prevalent. It is suspected that the BCN particle size is much smaller

than the analysis revealed, and it is probable that the manufacturer sizing is correct and refers to the smaller, fundamental particle size.

The purpose of this thesis was to investigate the burning rate characteristics of nano- and micron-sized metal oxide additives. These additives were added at a 4% level by weight and included aluminum oxide (Al_2O_3), ceria (CeO_2), and titania (TiO_2), each in their nano- and micron forms. Aluminum oxide and ceria were sourced from Sigma-Aldrich, and titania was sourced from Alfa Aesar. These specific additives were chosen because the Petersen Research Group has past experience with them and they have also been used as burning rate modifiers in former GN/BCN gas generant studies [16,22,23,25,51]. The results from this study build upon previous studies to better understand burning rate characteristics of nano- and micron-sized metal oxide additives. Additive mixtures were formulated by holding the ratio of GN/BCN constant (at stoichiometric) and simply making the additive 4% of the total mixture weight. Table 4 shows the seven mixtures this study explored. The baseline did not contain any additive and hence was used as the standard to compare all other formulations. The naming scheme is as follows: "μ" represents a mixture that has a micron-sized metal oxide additive, and "n" represents a nano-sized additive; this size designation is then followed by the additive that the formulation contains.

Table 4 Propellant formulations utilized in the present study

Formulation Name	Ingredient	% By Weight	Average Particle Size	Notes
baseline	guanidine nitrate	53.36	197.4 µm	-
	basic copper nitrate	46.64	98.33 µm	-
µ-Al_2O_3	guanidine nitrate	51.21	197.4 µm	-
	basic copper nitrate	44.79	98.33 µm	-
	micron aluminum oxide (Al_2O_3)	4	3 µm	gamma-phase
n-Al_2O_3	guanidine nitrate	51.21	197.4 µm	-
	basic copper nitrate	44.79	98.33 µm	-
	nano aluminum oxide (Al_2O_3)	4	20 nm	gamma-phase
µ-CeO_2	guanidine nitrate	51.21	197.4 µm	-
	basic copper nitrate	44.79	98.33 µm	-
	micron cerium oxide (CeO_2)	4	<5 µm	-
n-CeO_2	guanidine nitrate	51.21	197.4 µm	-
	basic copper nitrate	44.79	98.33 µm	-
	nano cerium oxide (CeO_2)	4	<50 nm	-
µ-TiO_2	guanidine nitrate	51.21	197.4 µm	-
	basic copper nitrate	44.79	98.33 µm	-
	micron titanium oxide (TiO_2)	4	44 µm (325 mesh)	anatase-phase
n-TiO_2	guanidine nitrate	51.21	197.4 µm	-
	basic copper nitrate	44.79	98.33 µm	-
	nano titanium oxide (TiO_2)	4	<25 nm	anatase-phase

3.2 Mixing Method

In section 2.5, Propellant Preparation Methods, several mixing techniques were described. There are essentially two ways to mix a propellant, dry or wet mixing. Dry mixing is usually done by hand or with a mechanical mixer. Wet mixing can also be done by hand or with a mechanical mixer and is best if spray dried after mixing, allowing the particle size to be consistent and controlled. A new method that has not been seen tested with airbag propellants before has been utilized for this study. The Petersen Research Group has recently acquired a Resodyn Resonant Acoustic Mixer (RAM), which was used for formulation mixtures. This machine uses high-energy and low-frequency acoustic waves, creating a uniform shear force, for mixing powders,

solids, liquids, gases, and mixtures thereof. Mixing intensity is measured in multiples of gravity (g's) at 60-Hz frequency, ranging from 1 to 100 g's. This mixer in particular can mix like or dissimilar powders, such as micron-micron powders and micron-nano powders, in a matter of minutes. The use of resonance mixing oscillates the entire system, transferring energy into the powders, creating oscillating mixing zones 50 microns in size [52]. This pattern quickly creates uniformly mixed formulations that would not otherwise be achieved. Resodyn has proven though SEM analysis that a micron-sized powder can be fully coated by a nanopowder using acoustic mixing [53]. Figure 10 displays a graphic of the resonance mixing technology used by Resodyn [52]. This technology allows for fast, reproducible formulations that can be done in fewer steps.

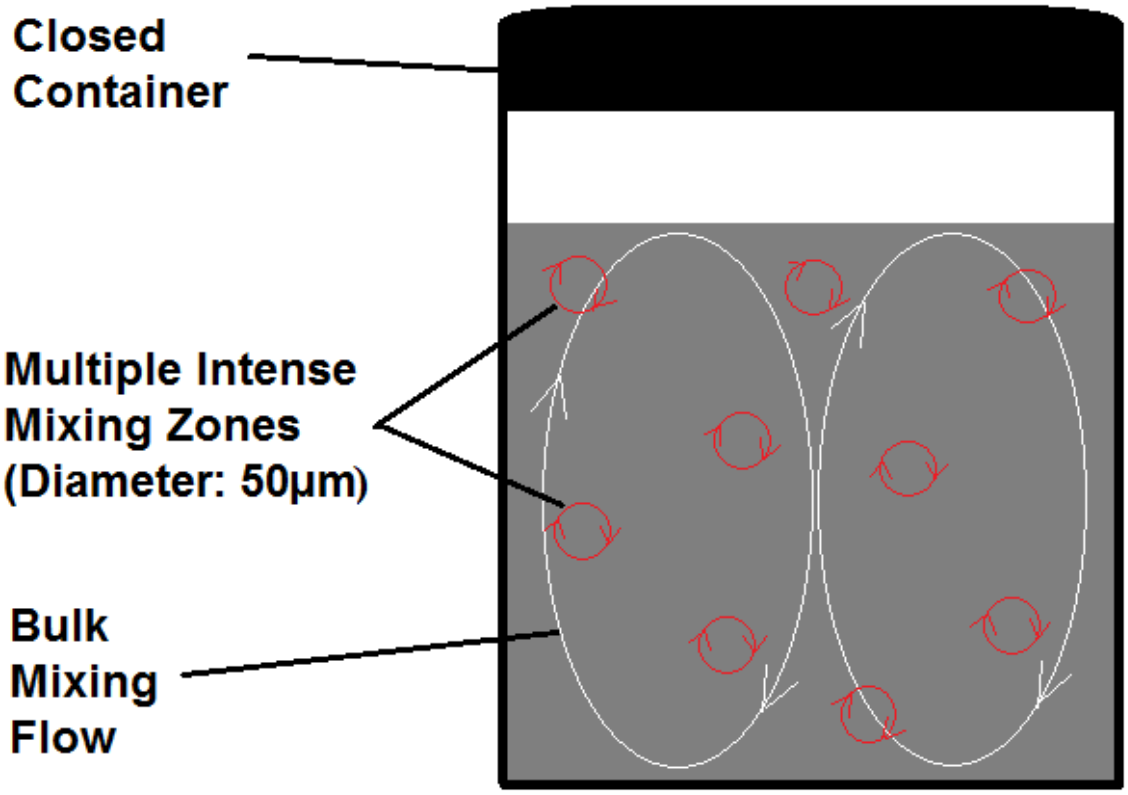

Figure 10 Acoustic mixing with large and micron-sized oscillating flow fields. Adapted from [52]

The Resodyn mixer is fairly simple to use and has only three main settings, mixing time, mixing intensity, and container fill level. To determine the optimal settings, literature was reviewed from previous mixing studies. Vanarase et al. [54] investigated mixing of two micron-sized powders and discovered that high fill level (75%), low acceleration (47 g's), and short mixing time (~1 minute) were best. If the fill level was low and the intensity high, powder stayed lofted in the dead space at the top of the container. High fill and high acceleration (82 g's) mixed faster and had comparable results to high-fill, low-acceleration mixtures. Relative standard deviation was used to

measure powder concentration for degree of mixture uniformity. Osorio and Muzzio [55] furthered Vanarase's study by mixing micron-sized acetaminophen with several other powders. They determined that better mixing was achieved with higher accelerations (70 g's). The container fill level did not have a significant impact, and mixing past two minutes did not have any further effect. Additional studies have shown successful mixing of energetic materials such as nanothermites, 3-nitro-1,2,4-triazole-5-one (NTO), and nitroguanidine (NQ) [56,57].

After comparing mixing settings from several studies, mixing parameters were chosen as follows: 2-minute mixing time, 70 g's of acceleration, and 75-85% fill. Formulations, per Table 4, were weighed and placed into 36-mL plastic vials for mixing. Figure 11and Figure 12 show the loaded Resodyn mixer and propellant before and after mixing, respectively. It is important to note that the micron-sized aluminum oxide was

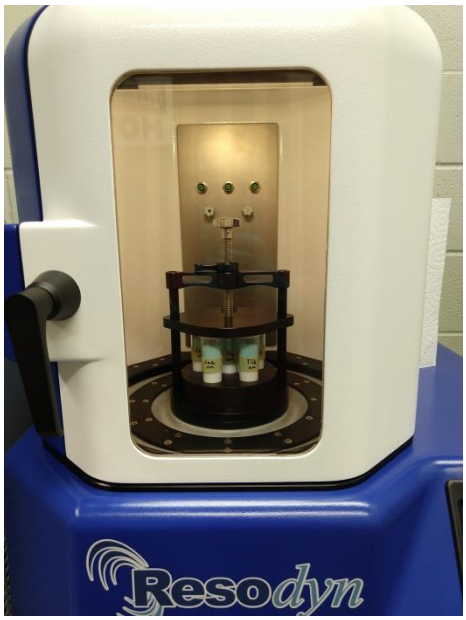

Figure 11 Resodyn Mixer

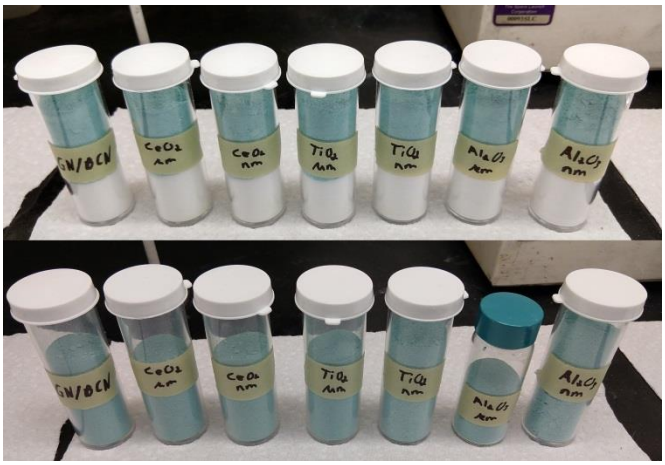

Figure 12 Propellant before (top) and after (bottom) mixing

very static, and mixing spread white spots of the additive onto the walls of the plastic vial. Although the rest of the mixture was uniform, some of the additive was stuck to the walls. To solve this problem, a smaller glass vial was used; this reduced static forces, and fully uniform mixing was achieved.

4. EXPERIMENTAL SETUP

4.1 Sample Preparation

With all of the formulations from Table 4 mixed, processing to form pellets was the next step. The first step in this pellet-formation process included weighing 3 g of powder into a custom-machined pellet punch, which was lubricated with dry PTFE lubricant spray. This device is made up of four main parts: the anvil, punch, die, and base. A cutaway of this device can be seen in Figure 13, showing propellant powder that has been pressed into a pellet. The pellet punch was machined from A10 tool steel,

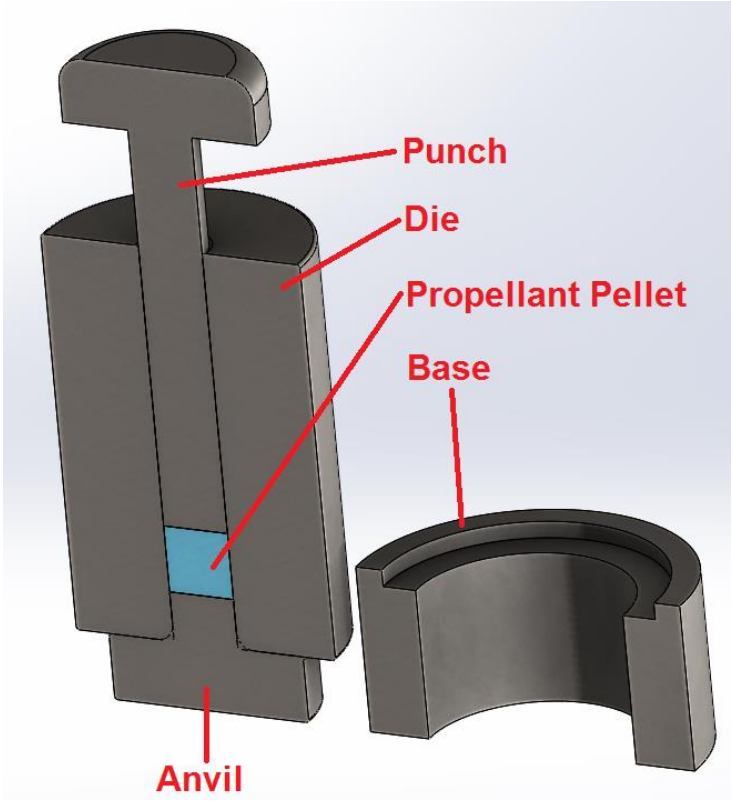

Figure 13 Computer generated pellet punch cutaway showing how a powdered propellant is pressed into a pellet

which was selected due to its easy machinability and its high metal on metal wear resistance. Heat treatment was also performed to increase its hardness to about 55 Rockwell C Hardness (HRC) to reduce potential for localized plastic deformation that could occur while pressing. The pellet punch components can be seen in Figure 14.

Figure 14 Pellet punch components

Once the pellet punch was filled with the specified amount of powder, it was then loaded into a Carver M-NE3890 hydraulic press. This programmable, touchscreen press has a clamping force of 50,000 pounds. To compact the pellets, the pellet punch was loaded between the platens and a program was set to press with 12,000 pounds of force for ten seconds. Once the cycle completed, the anvil was removed and the base was loaded between the platens and a program was set to press with 12,000 pounds of force for ten seconds. Once the cycle completed, the anvil was removed and the base was

placed under the die. The pellet punch was placed back between the platens and the press was closed slowly to carefully push the pellet out of the die. The press and loaded pellet punch can be seen in Figure 15 and Figure 16 respectively. The newly formed

Figure 16 Carver press

Figure 15 Pellet punch loaded between the platens of the press

pellet was then massed and measured. All pellets in the study had a final mass between 2.99 and 3.01 g. Their width was 0.5 inches and their height was also about 0.5 inches, with the smallest 0.4860 inches and largest 0.5050 inches. These measurements were later used to calculate pellet density and burning rate.

The next step was to prepare the pellets for burning. To get an accurate burning rate, the pellet was inhibited everywhere but the top surface. The inhibitor used was a spray paint acrylic enamel primer and was applied to the pellet twice. This procedure

allowed the pellet to experience a one-dimensional linear burning profile. If the sides were not painted, the pellet would burn on all surfaces, artificially increasing the burning rate and giving inaccurate results. The pellets, now ready for testing, were stored in a desiccator until each pellet was ready to burn.

4.2 Strand Burner and Data Acquisition

The burning rate characterization experiments were performed using a constant-volume strand burner with a custom-machined, sample-holding bolt. The strand bomb is about 1.15 liters in volume and is made of low-carbon steel alloy capable of testing up to 8,000 psi [58]. It was designed with four optical ports, three on the sides and one on the top. The top window is used for CO_2 laser ignition (not employed herein), and the three side windows can be used for several other diagnostic measurements such as high-speed video, mass spectrometry, and photoreceiver light emission. This pressure vessel can be seen in Figure 17.

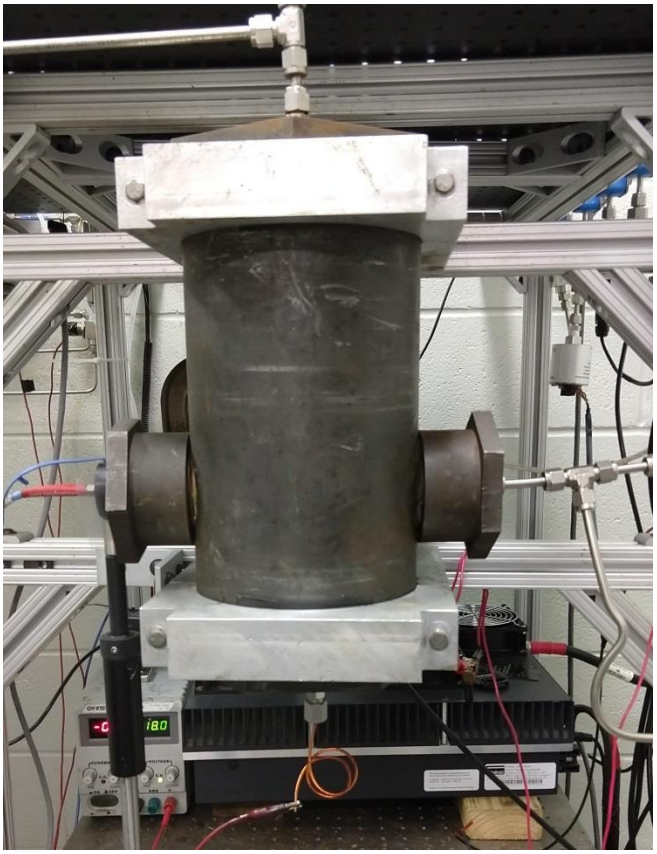

Figure 17 High-pressure, constant-volume testing vessel

The custom bolt was machined out of 316 stainless steel and screws into the bottom of the strand burner for testing and quickly replacing each propellant sample. There is a copper Conax ignition lead that runs through the bolt for ignition. A Viton o-ring ensures a leak-free seal. Figure 18 displays the custom bolt described, and a machine drawing of the piece is available in Appendix A. A nichrome wire was used for ignition by running 18 volts at 7.5 amps through the wire, igniting the propellant. The top of the propellant was first wrapped with a quarter-inch-wide piece of tape used to hold highly energetic black ignition powder (boron, potassium nitrate mixture) on top of the pellet. The pellet was placed into the slot on top of the bolt, and then a nichrome wire

Figure 18 Bolt used to hold the propellant sample for testing

was wrapped around the ignition and ground leads and placed over the surface to the propellant. The black powder (0.11 g) was then evenly spread over the top of the pellet so that once ignition occurred, the entire top surface of the pellet would ignite uniformly, creating a linear burn. Tape was then placed and pressed over the ignition powder so that it would not be displaced while pressurizing the vessel. Figure 19 shows the sample loading process from once the pellet is pressed to when it is ready to be inserted into the strand burner for testing.

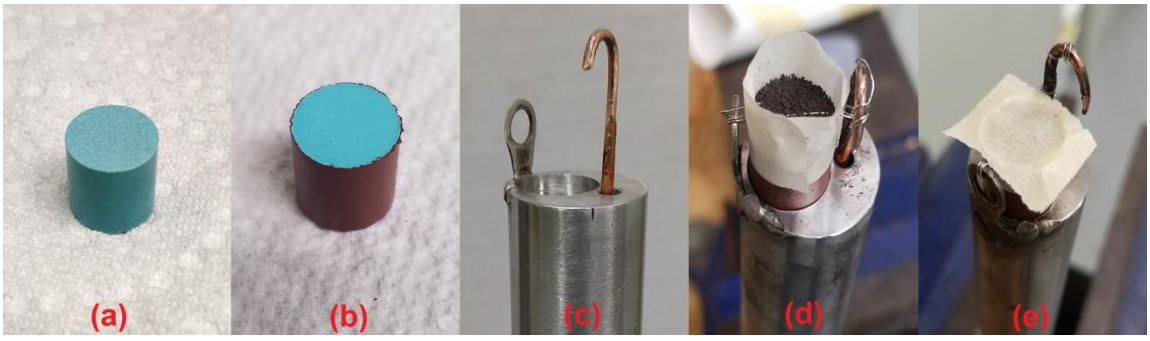

Figure 19 Pressed sample loading process. A pressed sample (a) was painted (b) and placed into the custom bolt cutout (c) where tape was wrapped around the top, ignition powder was loaded, and a nichrome wire was connected across the leads (d). Lastly, tape was pressed over the top to secure the powder (e)

Once the sample was loaded onto the bolt and secured in the strand burner, safety checks were performed and the data acquisition (DAQ) software was booted up. The strand burner, located in a test cell in the Turbomachinery Laboratory building, has steel-reinforced concrete walls and a blast-proof door. The control room, separate from the test chamber, contains DAQ computer systems and a control board for remote pressurization and ignition. Nitrogen was used as the inert pressurizing gas, and three pressure transducers track any pressure changes. The first transducer was used to send information to GageScope, a program which records voltage signals from the Gage Applied Sciences DAQ board. The second and third transducers sent digital readings to the user control board. One of these transducers was used for calibration and was not normally exposed to exhaust gasses. Two pneumatic valves were used, one to control the nitrogen fill flow and another to control the test vessel exhaust flow. Spectrometry via an Ocean Optics spectrometer, light emission via a Si photodiode from New Focus, and high-speed video via a Photron FASTCAM SA3 120K camera were also sent to a DAQ computer system. The test facility setup can be seen in Figure 20. Further information on the test facility can be found in papers by Carro et al. [58,59].

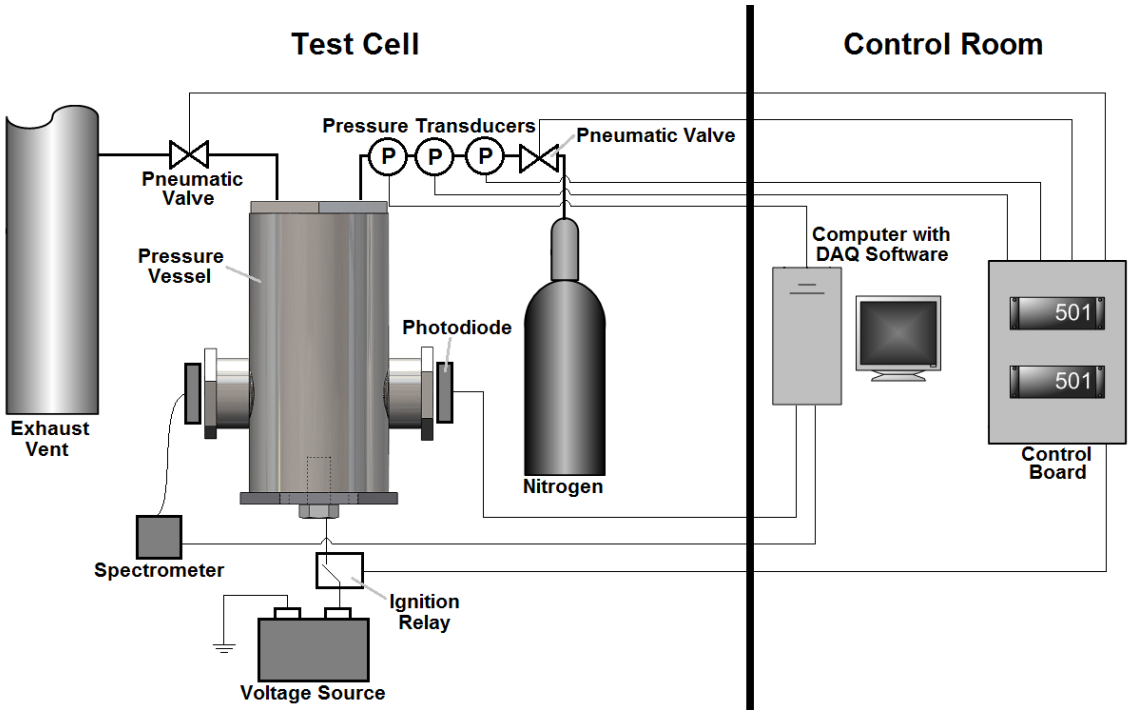

Figure 20 Test facility experimental setup. High speed camera (not shown) located behind pressure vessel and connects to computer

Testing was then conducted, and data were recorded for each of the formulations. Each formulation was tested at four pressures: 1000, 2000, 3000, and 4000 psi. At least four samples, one for each pressure, were tested. A couple of extra samples in each formulation were made to retest any suspect data points.

5. RESULTS AND DATA ANALYSIS

5.1 Material Properties

Before the formulations were tested, chemical properties were gathered and used to calculate several important combustion characteristics, such as adiabatic flame temperature, theoretical density, molecular weight of the products, and gas yield. The chemical properties were gathered from several sources, and propellant evaluation software based on equilibrium thermochemistry, ProPEP, was utilized to perform most of the calculations. Table 5 displays these properties. Chemical properties for GN,

Table 5 Chemical properties used for theoretical calculations

Chemical	Molecular Weight (g/mol)	Density (g/cc)	Heat of Formation (cal/g)
GN	122.08	1.44	-758
BCN	480.22	3.41	-867
Al_2O_3	101.96	1.85	-4000
CeO_2	172.12	7.13	-1512
TiO_2	79.87	4.23	-2551

aluminum oxide, and titania were readily available in ProPEP and were confirmed by Autoliv, the project industry partner. Properties for BCN were difficult to find, but molecular orbital package (MOPEC) software held this information under another name for BCN, copper trihydroxide nitrate, and these properties were also confirmed by Autoliv. Lastly, ceria thermodynamic properties were not available in ProPEP, NASA CEA, or in the JANAF thermochemical tables but were found in a U.S. geological survey bulletin [60].

These chemical properties were then used to characterize the combustion of each formulation. Theoretical density was calculated and compared to the average actual density of pellets from each formulation as seen in Table 6. It can be seen that the actual

Table 6 Density and adiabatic flame temperature of the tested formulations

Formulation Name	Theoretical Density (g/cc)	Actual Density (g/cc)	Density Difference (%)	Adiabatic Flame Temperature (K)
baseline	1.967	1.856	-5.66	1898
μ/n-Al_2O_3	1.963	1.864	-5.03	1841
μ/n-CeO_2*	2.026	1.906	-5.93	1885
μ/n-TiO_2	2.011	1.870	-6.99	1889

*Theoretical density and adiabatic flame temperature calculated by hand

density is only about 5% to 7% lower than the theoretical density in each case. It is ideal to be as close to theoretical as possible to ensure accurate results. The sample pellets were solid without any visible voids or cracks and were all very close in mass and volume within each formulation. If voids were present the density would be lower than expected, and these pockets would artificially increase the burning rate due to a sudden increase in surface area. A more-stringent pressing procedure could be used to reduce this density difference, possibly one with multi-step force increments similar to the procedure performed by Ulas et al. [10]. The adiabatic flame temperature was also calculated and the results were as expected, with the stoichiometric mixture having the highest flame temperature and each additive decreasing it slightly. It is important to note that theoretical density and adiabatic flame temperature for ceria were calculated by hand since ProPEP did not contain thermochemical data for this chemical. The same equations that ProPEP uses were done by hand instead. Adiabatic flame temperature was

calculated by setting the enthalpy of the reactants equal to the enthalpy of the products, $H_r=H_p$, and solving the equation iteratively until it converges to a single temperature. To confirm accurate calculations, the adiabatic flame temperature was first calculated for the aluminum oxide formulation by hand with a final result of 1866 Kelvin, which is only 25 Kelvin or 1.36% error from the program calculation. This percent error is quite low, so it was concluded that the adiabatic flame temperature calculation for the ceria formulation was accurate. Additionally, the molecular weight of the products and the gas yield were calculated with results in Table 7. Again, ceria values were calculated by hand and confirmed accurate by first correctly calculating these values from other formulations and matching ProPEP results.

Table 7 Combustion product properties

Formulation Name	Molecular Weight of Products (g/mol)	Gas Yield (moles/100g)
baseline	29.449	3.011
μ/n-Al_2O_3	30.316	2.890
μ/n-CeO_2*	30.417	2.888
μ/n-TiO_2	30.222	2.890

*Values calculated by hand

5.2 Burning Rates

To infer the burning rate of a propellant sample from the experiment, two main pieces of information were required: sample length and burn time. Once this information was known, the burning rate could be calculated by simply dividing sample length by burn time as seen in Section 1.2, Equation 1. Measuring the length of the pellet was easily done with digital calipers, but burn time had to be experimentally determined.

Several tools were used to determine the start and end of the burn. Pressure trace, light trace, and high-speed video were all diagnostic tools used to accurately measure the burn time. Burn time being extracted from a pressure and light trace can be seen in Figure 21.

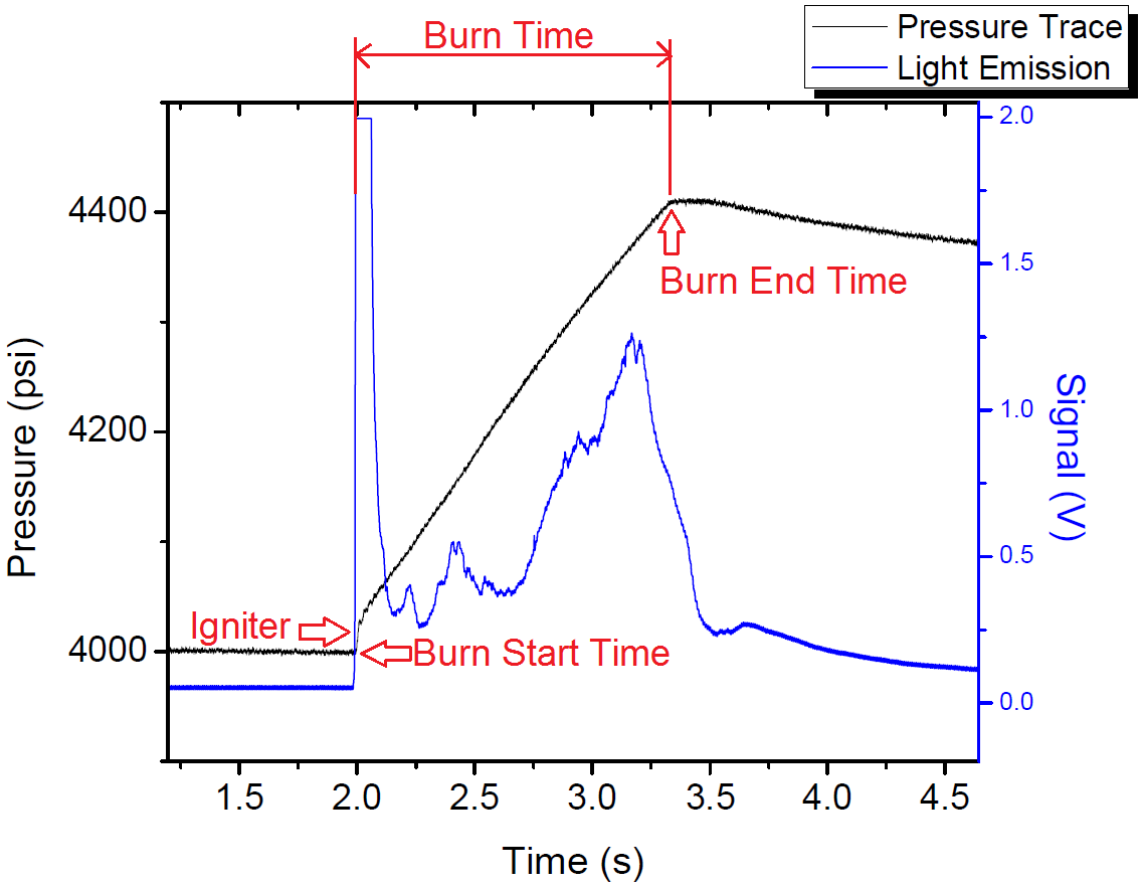

Figure 21 Burn time extracted from pressure and light trace. Trace shown is μ-CeO_2 at 4000psi

From the pressure and light curves, the burn start time could be definitively determined. The pressure trace showed an initial, almost vertical jump in pressure rise which was the highly energetic black powder igniter lighting. The igniter powder evenly ignites the top surface of the propellant, which could then be seen to have a linear burn. The burn start time was clear in the light trace as well, with a vertical rise after light was emitted from

the ignitor powder. High speed video also confirmed the burn start time, with a visible flash of light from the ignition powder. The burn end time was routinely very clear in the pressure curve, but somewhat vague if just using the light curve or high speed video. Since these propellants would smolder at the end of their burn, light was still being emitted from the propellant after the burn had ended. It could be seen from the pressure curve that the burn end time was where the linear increase of pressure ended.

After all sample lengths and sample burn times were recorded, burning rates were calculated for each test. This information as well as pressure rise is displayed in Table 8. To examine these results further, burning rate curves for each formulation were constructed and inspected. These results are contained in the following section.

Table 8 Experimentally determined burning rates and pressure rise

Formulation Name	Burning Rate (in/s) (% Difference from Baseline)				Pressure Rise (psi) (% Rise)			
	1000 psi	2000 psi	3000 psi	4000 psi	1000 psi	2000 psi	3000 psi	4000 psi
baseline	0.2152	0.2640	0.3113	0.3610	246 (24%)	329 (16%)	393 (13%)	442 (11%)
μ-Al_2O_3	0.2142 (-0.5%)	0.2608 (-1.2%)	0.2919 (-6.2%)	0.3294 (-8.8%)	232 (23%)	306 (15%)	379 (13%)	414 (10%)
n-Al_2O_3	0.2013 (-6.5%)*	0.2500 (-5.3%)*	0.2888 (-7.2%)	0.3110 (-13.9%)	217 (22%)*	302 (15%)*	363 (12%)	401 (10%)
μ-CeO_2	0.2190 (1.8%)	0.2695 (2.1%)*	0.3257 (4.6%)	0.3614 (0.1%)	238 (24%)	314 (16%)*	366 (12%)	411 (10%)
n-CeO_2	0.2028 (-5.8%)*	0.2520 (-4.5%)*	0.2993 (-3.9%)	0.3462 (-4.1%)	234 (23%)*	304 (15%)*	365 (12%)	416 (10%)
μ-TiO_2	0.1974 (-8.3%)*	0.2476 (-6.2%)*	0.2976 (-4.4%)	0.3373 (-6.6%)	232 (23%)*	305 (15%)*	365 (12%)	416 (10%)
n-TiO_2	0.1820 (-15.4%)*	0.2447 (-7.3%)*	0.2952 (-5.2%)	0.3286 (-9.0%)	220 (22%)*	301 (15%)*	359 (12%)	413 (10%)
*Average of two points								

5.3 Burning Rate Curves

Burning rate curves are used to approximate the burning rate of a solid propellant as a function of pressure using St. Robert's law or Vieille's law as seen in Equation 5 [1]. When the burning rate was plotted against pressure on a log-log scale, a linear relationship formed.

$$r = aP^n \quad \textbf{(5)}$$

In this equation, *r* represents the burning rate, *a* represents the temperature coefficient, *P* represents the pressure, and *n* represents the pressure exponent. The temperature coefficient accounts for variation in the sample initial temperature. The pressure exponent is also known as the combustion index and provides information about chamber pressure sensitivity. If the combustion index is greater than one, any disturbance in pressure will be amplified in the chamber. This event is undesirable and in particular for airbag gas generants, an index below 0.35 is advantageous [20].

To determine the burning rate curve equation for each formulation, the burns were plotted on a log-log scale, and a power curve fit revealed this equation. These burning rate curves can be seen in Figure 22, Figure 23, and Figure 24 which compare aluminum oxide, ceria, and titania, respectively, to the baseline.

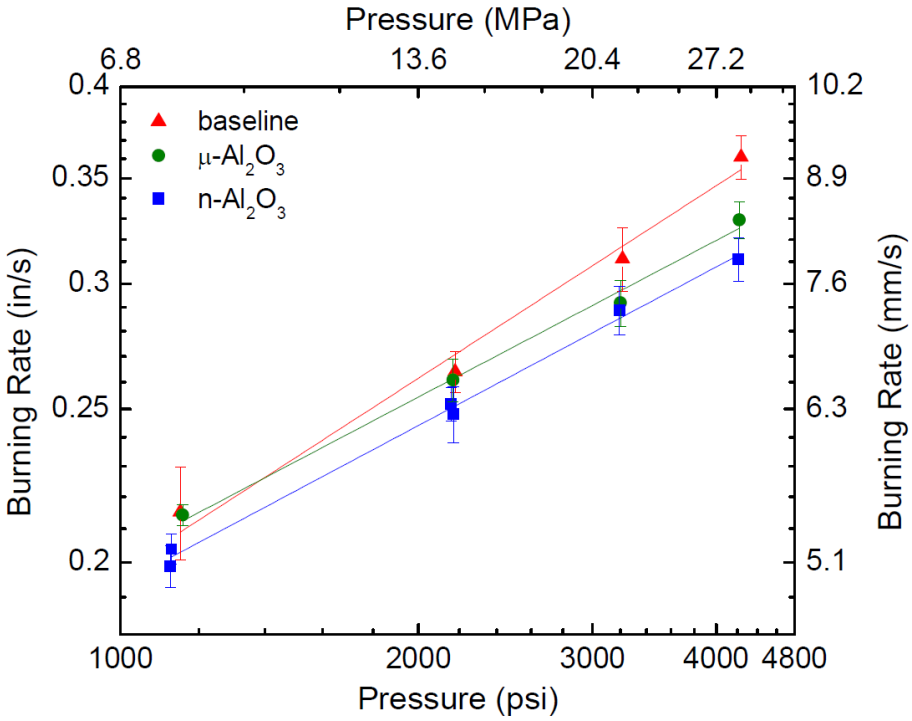

Figure 22 Aluminum oxide burning rate curves

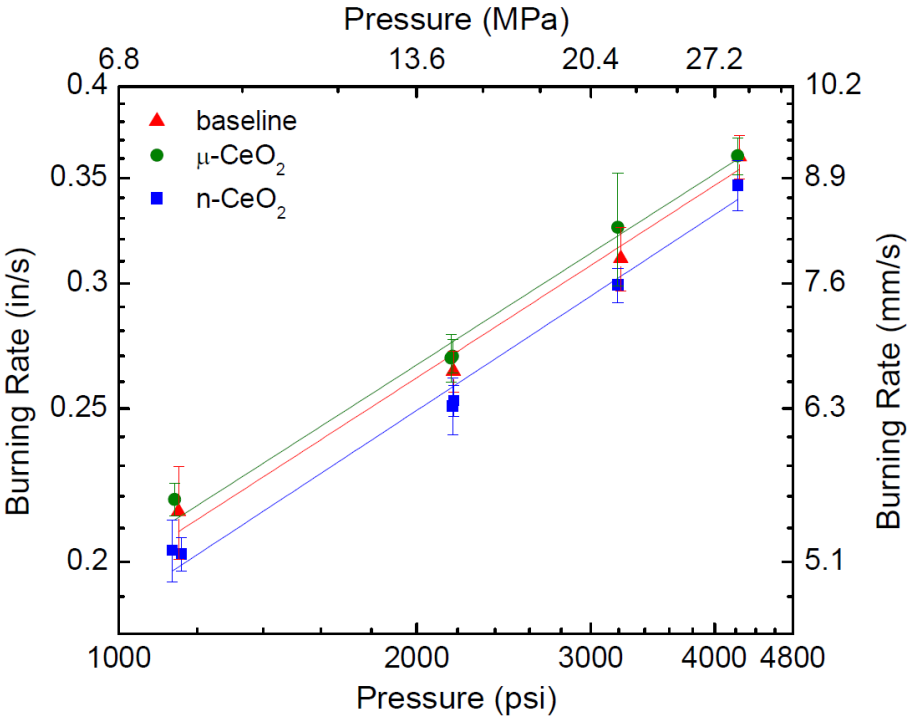

Figure 23 Ceria burning rate curves

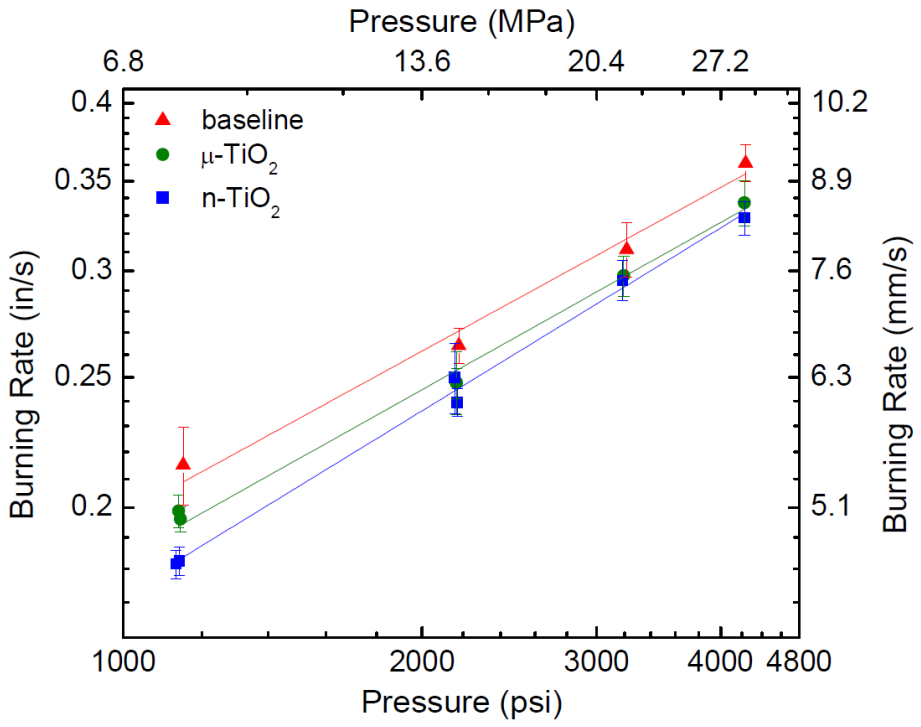

Figure 24 Titania burning rate curves

From Table 8 and the above three figures, all but the micron ceria formulation decreased the burning rate when compared to the baseline. It is also important to note that for all three additives, their nano-form performed worse than their micron form. To further evaluate the data, Table 9 shows the experimentally determined values for Equation 5. The pressure exponent corresponds to the slope of each curve on a log-log scale and relates to the pressure dependence of a propellant, which is desired to be low. Compared to the baseline, aluminum oxide performs the best in this aspect, having the lowest value for *n*. Both ceria formulations and micron titania do not significantly affect the pressure exponent, while nano titania increases it the most. If low pressure dependence was the goal for this propellant, aluminum oxide would be best out of these

Table 9 Experimentally determined burning rate equation variables

Formulation Name	Pressure Exponent (n)	Temperature Coefficient (a)	R-Squared
baseline	0.41	0.01202	0.980
μ-Al_2O_3	0.33	0.02077	0.990
n-Al_2O_3	0.33	0.01930	0.995
μ-CeO_2	0.40	0.01254	0.986
n-CeO_2	0.41	0.01087	0.985
μ-TiO_2	0.41	0.01051	0.992
n-TiO_2	0.45	0.00756	0.994

additives, although it does decrease the burning rate. Titania performed worst in both burning rate and pressure exponent reduction, with its nano-sized form the worst overall additive. Ceria was seen as the best additive overall, with its micron-sized form displaying the best characteristics. Although it does not affect the pressure exponent, micron-sized ceria was seen to slightly increase the burning rate when all other additives suppressed it. R-squared values are also near one, meaning that the data points are closely related to the expected power curve model used for solid propellants on a log-log scale.

Combustion slag was also recovered and qualitatively examined after each test. The baseline and each additive had unique slagging properties, with micron- and nano-sized differences for each respective additive not having an effect. The baseline, ceria, and titania formulations all produced very rigid and tough slag. The baseline slag was highly amorphous and would result in a different-shaped droplet each time. Aluminum oxide formulations produced cylindrical-shaped slag which was rigid with many small internal voids, and it would crumble if a small amount of force was exerted on it. Ceria formulations produced a small mound with internal voids, but would not break unless a

considerable amount of force was exerted. Titania slag was very interesting since it would create a hollow circle or crescent without voids that would also not easily break. The recovered slag can be seen in Figure 25. The slagging properties of aluminum oxide coincide with data seen in another study in which a similar propellant was used, and 4% loading of aluminum oxide produced 57.1% solid slag recovery [16].

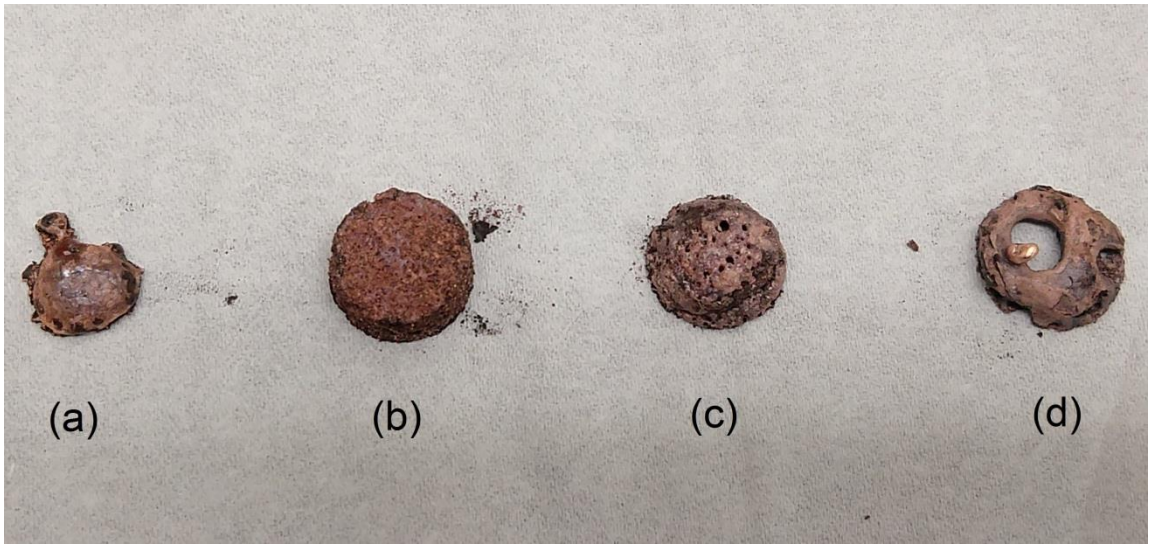

Figure 25 Typical slag recovered from (a) baseline, (b) aluminum oxide, (c) ceria, and (d) titania formulations

The results from this study were not as initially expected. Most of the additives decreased performance, and nano-sized additives performed worse than micron-sized additives. Though nano- versus micron-sized additives have not been studied with guanidine base propellants, it has been seen in AP/HTPB propellants that nano-sized additives can have lower performance than their micron-sized counterparts. Stephens et al. [22] determined from SEM imaging that agglomerations in the nano-additives were present and that a better mixing could increase dispersion and increase the burning rate.

However in all cases, propellant performance was increased. Increased performance was only observed in one formulation in this study.

Other GN/BCN studies with similar weight ratios have observed increased burning rates from aluminum oxide as an additive [25,38]. These studies show a baseline GN/BCN ratio of 52.13:47.87 having a burning rate of 0.28 inches per second. Aluminum oxide added at 2.5% and 3% showed burning rates of 0.55 and 0.50 inches per second, respectively. The burning rates of these two additive levels were gathered over two separate studies and preparation methods were not detailed, but it is seems that as the percent of aluminum oxide increased, the burning rate decreased slightly. This leads to the idea that a 4% additive loading may be too high, but this level was chosen from a concentration study conducted on another additive in collaboration with an industry partner, Autoliv. The most promising conclusion is more complex and deals with not just the particle size of the additive, but the particle sizes of GN and BCN as well.

Described in Section 2.6, the particle sizes of fuels and oxidizers are seen to range significantly in different studies. It was observed that as the size of BCN decreased, the burning rate increased in GN-based propellants [9]. Furthermore, desired fuel and oxidizer particle sizes in several patents range from several hundred microns to less than one micron; but the patents are in agreement that as the particle size is decreased, increased performance is expected [4,20,49]. Additionally, Mei et al. [7] conducted thermal decomposition experiments on GN/BCN/Fe_2O_3 and discovered that the onset of reaction of GN/Fe_2O_3 takes place at 257.9 °C, which is higher than the

temperature at the end of the GN/BCN/Fe_2O_3 reaction, about 250 °C. It was concluded that iron oxide must have interacted mainly with the BCN and more specifically the Cu or CuO produced from the combustion of GN/BCN. It is also noteworthy that iron oxide increased the thermal stability but decreased the burning rate. If the metal oxide additives in the present study behave in a similar way, then it is possible that the size of BCN plays an important role in the burning rate and the decrease due to additives. It is not clear from the literature if ceria and titania should increase the burning rate when compared to a GN/BCN baseline, but aluminum oxide should.

With the information known about BCN size and that iron oxide acts primarily on the oxidizer BCN, a similar mechanism has been described by Kreitz et al. [61] in AP/HTPB propellants where similarly the additive catalyzes the oxidizer. In the Kreitz et al. [61] study, propellants were tested with monomodal and bimodal AP with a nano-sized titania additive. Monomodal AP consisted of average particle sizes of 200 microns and bimodal AP consisted of 70%, 200-micron and 30%, 20-micron particle sizes. Results revealed that the bimodal AP formulation performed worse than monomodal. The authors further explain that the additive is only as effective as the number of reaction zones created and can be described by f_c, the fraction of reactions catalyzed. Equation 6 shows the authors proposed a relationship between the fraction of reactions catalyzed, the additive agglomerate size, D_{Agg}, and AP size, D_{AP} [61].

$$f_c = 1 - f\left(\frac{D_{Agg}}{D_{AP}}\right)_i \quad \textbf{(6)}$$

The additive must catalyze the reaction between AP and HTPB, but in the bimodal formulation, due to the addition of fine AP, many more AP/HTPB reaction zones are

created while the additive is still only able to effectively catalyze the number of zones originally present in the monomodal formulation. The additive dispersion is limited due to agglomerations and additional reaction zones are not created.

A similar analysis can be conducted on formulations in this study. The size distribution of BCN previously analyzed in Figure 8 ranges widely from less than one micron up to one thousand microns. The particle analysis data differed from the manufacturer, which stated that the D90 was 10.82 microns as compared to 216.5 microns from the analysis. Whether this discrepancy is due to inaccurate manufacturer data or BCN particle agglomeration, the same conclusions can be made. The nanoparticle additives are not able to catalyze as many reaction zones and are instead just leeching some of the heat from the reaction and reducing the burning rate. On the other hand, the micron-sized additives are doing this negative contribution to a lesser extent, with ceria being the exception. More reaction zones are catalyzed since some of the oxidizer particles are actually smaller than the additives, thus creating additional reaction zones around the additive instead. In this case, Equation 6 does not hold since the additive size is actually larger than the oxidizer, creating a negative fraction of reactions catalyzed. A visual representation of this relative size effect can be seen in Figure 26 where the nano-sized additive is more abundant but ultimately creates fewer catalyzed reaction zones than the micron-sized additive.

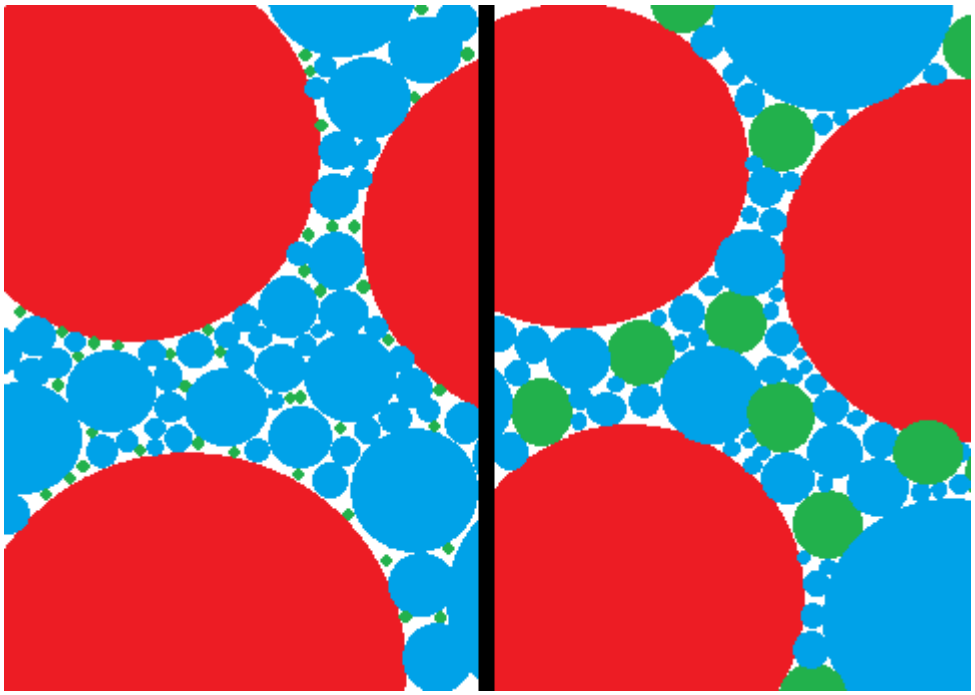

Figure 26 GN represented as red, BCN as blue, and additive as green. Nano-sized additive formulations (left) form fewer catalyzed reaction zones than micron-sized additives (right) due to large particle size distribution of BCN

If this scenario is in fact what is occurring, then there are several parameters that could be changed to more effectively compare nano- and micron-sized metal oxide additives. The first parameter would be to better control the size of BCN and GN, decreasing the particle size of both for increased burning rate and allowing for a more accurate assessment of nanoparticle effectiveness. Additionally, agglomerations should be reduced to a minimum, possibly by reducing atmospheric moisture and ultrasonic mixing. Lastly, an additive concentration study should be conducted for each metal oxide to determine the optimal weight percentage to use for the comparative experiments.

5.4 Uncertainty Analysis

When conducting experiments, uncertainty is inevitable and it can come from many sources ranging from instrument accuracy to human error. Measurements taken during the pellet preparation process and data collection during testing can create error. During pellet preparation, the length and mass of each pellet were measured with an accuracy of ±0.0005 inches and ±0.01 g, respectively. When conducting experiments, pressure transducer accuracy, as reported by the manufacturer, is 0.15%. This inaccuracy correlates to ±1.5 psi for tests conducted at 1000 psi and ±6.75 psi for tests where pressures reach 4500 psi.

Uncertainty in the burning rate combines more than one parameter and can be calculated using the root-sum-square (RSS) method. The burning rate depends on the length of the sample as well as the burn time as seen previously in Equation 1. This calculation requires manual selection of a burn start and end time as described in Figure 21. Utilizing the pressure trace, light trace, and high-speed video, selection of the burn start and end time can be accomplished with high accuracy and repeatability. Error in this method arises from what an individual considers the burn start and burn end times. Defined by our industry partner Autoliv, the burn start and end times are when the rate of change of the rate of change, or the second derivative, is greatest. This definition corresponds to the beginning of the initial spike from the ignition powder for the start time and when the linear pressure rise begins to level out for the end time. This method assumes that the pellet begins burning almost instantaneously after the ignition powder lights and that the burn ends just as the linear pressure rise finishes. If the pressure curve

is smooth and the burn is linear as expected, then an individual can use the industry burn time method to select these points with less than a 1% error in burning rate. Larger sources of error are presented from two main sources: combustion fluctuations/non-linear burning and an individual's definition of burn start and end time. Combustion fluctuations can lead to a pressure trace that is not smooth, with burn start and end time graphic features that are not well defined. Also, an individual may believe the burn actually starts after the initial ignition-powder pressure spike and ends at the point of maximum pressure. It is difficult to know the exact time the pellet fully ignites due to the explosive nature of the ignitor powder. It is also difficult to know the exact time the burn ends due to smoldering. In both these cases, the minimum and maximum burning rate error in these sets of experiments was found to be 1.52% and 8.14% respectively. The average error in burning rate for all data points is 3.37%.

Density requirements are also important and should be as close to the theoretical density as possible. If the actual sample density if much lower than the theoretical, voids and cracks may be present in the propellant that could cause an artificially increased burning rate. Propellant densities in this study were found to be about 5% to 7% of theoretical, which is within an acceptable range. Furthermore, multiple samples within the same formulation were tested at the same pressure to ensure similar burning rates. Nine samples were tested twice at their same respective test pressures, and their burning rates were found to vary by an average of only 1.34%. This variation can be attributed to combustion fluctuations and possibly outer-wall inhibitor inconsistencies.

6. CONCLUSION AND RECOMMENDATIONS

Burning rate characterization was performed on GN/BCN propellants which were loaded with nano- or micron-sized metal oxide additives. To best create an experiment to compare these burning rate characteristics for the first time at Texas A&M University, a detailed review of solid propellants and how they are used as gas generants in automotive airbags was conducted. This review included data on GN/BCN propellants, additives, preparation methods, and particle size effects. A detailed sample preparation method and experimental design were established.

Three metal oxide additives were chosen to test, each in their nano- and micron-sized forms. They were prepared and pressed into cylindrical pellets, similarly done in industry, and burning rate measurements were acquired. It was determined that all but one additive formulation decreased the burning rate from the GN/BCN stoichiometric baseline. The one exception was micron-sized ceria, which increased the burning rate compared to the baseline. Additionally, for every metal oxide, the nano-form reduced the burning rate further than the micron-form. These results were not initially as expected, but further analysis revealed a few possible conclusions. From the very different slag recovered from each additive formulation, it is clear that each additive is affecting the propellant in a different way. Although ceria and titania burning rate characteristics are not as well known in GN/BCN propellants, it was assumed that aluminum oxide should increase the burning rate, but this was not seen in the present study.

It has been reported by others that the size of GN and BCN are important and that reducing their size can lead to increased burning rates. Furthermore, a thermal decomposition study from the literature with iron oxide revealed that the additive primarily acts on the propellant oxidizer, BCN. Similar decomposition behavior has been seen in the Petersen Research Group with AP/HTPB propellants. It is theorized that due to the wide distribution size of BCN the number of catalyzed reaction zones for the nano-sized additives were actually reduced. At this point, the additive was no longer an effective catalyst and only removed heat from the main GN/BCN reaction. This mechanism occurs to a lesser extend with the micron-sized additives, which are thought to have more reaction zones due to the small-sized BCN coating the additive and creating more zones.

Future work recommendations include reducing the size of both GN and BCN and better controlling their particle size, especially for BCN. Agglomerations should be kept at a minimum by reducing any sources of moisture and using a mixing method which utilized ultrasonic waves to break up the agglomerations. An additive concentration study should also be conducted for each additive tested to determine the optimal additive level. Lastly, an incremental pellet pressing procedure should be utilized to bring the actual pellet density as close to the theoretical density as possible.

REFERENCES

[1] Sutton GP, Oscar Biblarz. Rocket Propulsion Elements. 9th ed. New Jersey: John Wiley & Sons, Inc.; 2017.

[2] Meyer R, Köhler J, Homburg A. Explosives. 6th ed. Weinheim: Wiley-VCH Verlag GambH & Co. KGaA; 2007.

[3] Lund GK, Blau RJ. Anhydrous 5-Aminotetrazole Gas Generant Compositions and Methods of Preparation. US Patent 5500059, 1996.

[4] Lundstrom NH, Shaw GC. Pyrotechnic Non-Azide Gas Generants Based on a Non-Hydrogen Containing Tetrazole Compound. US Patent 4370181, 1983.

[5] Khandhadia PS, Burns SP. Thermally Stable Nonazide Automotive Airbag Propellants. US Patent 6306232 B1, 2001.

[6] Engelen K, Lefebvre MH. Properties of Gas-Generating Mixtures Related to Different Fuel and Oxidizer Compositions. Propellants, Explos Pyrotech 2003;28:201–9.

[7] Mei X, Yang H, Li X, Li Y, Cheng Y. Study of Some Low Temperature Gas-Generating Compositions. Propellants, Explos Pyrotech 2015;40:526–30.

[8] Yamato Y. Gas Generating Composition. US Patent 2009/0211671 A1, 2009.

[9] Seo YD, Chung SH, Yoh JJ. Automotive Airbag Inflator Analysis Using the Measured Properties of Modern Propellants. Fuel 2011;90:1395–401.

[10] Ulas A, Risha GA, Kuo KK. Ballistic Properties and Burning Behaviour of an Ammonium Perchlorate/Guanidine Nitrate/Sodium Nitrate Airbag Solid Propellant. Fuel 2006;85:1979–86.

[11] Ulas A, Kuo KK. Laser-Induced Ignition of Solid Propellants for Gas Generators. Fuel 2008;87:639–46.

[12] Damse RS. Studies on the Decomposition Chemistry of Triaminoguanidine Azide and Guanidine Nitrate. J Hazard Mater 2009;172:1383–7.

[13] Mendenhall IV. Guanylurea Nitrate in Gas Generation. US Patent 6550808 B1, 2003.

[14] Nakashima M, Itaura T, Matsunaga H, Higashi E, Takagi S, Katoh K. A Fundamental Study on the Thermal Decomposition and Combustion Behaviors of Guanidine Nitrate and Basic Copper Nitrate Mixture. J Therm Anal Calorim 2018;131:95–100.

[15] Mei X, Cheng Y, Li Y, Zhu X, Yan S, Li X. Thermal Decomposition Properties of Guanidine Nitrate and Basic Cupric Nitrate. J Therm Anal Calorim 2013;114:131–5.

[16] Mendenhall IV., Taylor RD, Barnes MW, Parkinson DW. Burn Rate-Enhanced Basic Copper Nitrate Containing Gas Generant Compositions and Methods. US Patent 6143102, 2000.

[17] Barnes MW, Smith RG. Method for Preparing Pyrotechnics Oxidized by Basic Metal Nitrate. US Patent 2004/0173922 A1, 2004.

[18] Struble DE. Airbag Technology: What it is and how it came to be. Detroit: 1998.

[19] Meyer R, Köhler J, Homburg A. Explosives. 7th ed. Weinheim: Wiley-VCH Verlag GambH & Co. KGaA; 2015.

[20] Zeuner S, Schropp R, Hofmann A, Rodig K-H. Nitrocellulose-Free Gas-

Generating Composition. US Patent 2003/0145926 A1, 2003.

[21] Maggi F, Milano P, Deluca LT, Milano P. Nano vs. Micro Catalyst Effects on Solid Rocket Propellants. AIDAA Int. Conf., Milano: 2009.

[22] Stephens MA, Petersen EL, Carro R, Reid DL, Seal S. Multi-Parameter Study of Nanoscale TiO2 and CeO2 Additives in Composite AP/HTPB Solid Propellants. Propellants, Explos Pyrotech 2010;35:143–52.

[23] Lund GK, Bradford R. High Performance Gas Generating Compositions. US Patent 8815029 B2, 2014.

[24] Barnes MW, Taylor RD. Gas Generant Compositions Containing Amine Nitrates Plus Basic Copper (II) Nitrate and/or Cobalt (III) Triammine Trinitrate. US Patent 5608183, 1997.

[25] Mendenhall IV. Gas Generation via Metal Complexes of Guanylurea Nitrate. US Patent 6602365 B1, 2003.

[26] Huertas M. Gas Generating Compositions for Automotive Use Manufactured by Pellet Formation. International Publication WO 2007/012348 A1, 2007.

[27] Safety Data Sheet: Guanidine Nitrate. Sigma-Aldrich 2014;Ver 4.5. https://www.sigmaaldrich.com/Graphics/COfAInfo/SigmaSAPQM/SPEC/23/234249/234249-BULK_____ALDRICH__.pdf.

[28] USCAR24 Inflator Technical Requirements and Validation. Soc Automot Eng 2013.

[29] Oxley JC, Smith JL, Naik S, Moran J. Decompositions of Urea and Guanidine Nitrates. J Energ Mater 2009;27:17–39.

[30] Engelen K, Lefebvre MH, De Ruyck J. Combustion Properties of Gas-Generating Pyrotechnics. Combust Sci Technol 2001;163:49–76.

[31] Mendenhall IV., Barnes MW. Burn Rate Enhancement via a Transition Metal Complex of Diammonium Bitetrazole. US Patent 6712918 B2, 2004.

[32] DeLuca L, Caveny LH, Ohlemiller TJ, Summerfield M. Radiative Ignition of Double-Base Propellants. I. Some Formulation Effects. AIAA J 1976;14:940–6.

[33] DeLuca L, Ohlemiller TJ, Caveny LH, Summerfield M. Radiative Ignition of Double Base Propellants: II. Pre-ignition Events and Source Effects. AIAA J 1976;14:1111–7.

[34] Kuo KK, Kim JU, Fetherolf BL, Torikai T. Preignition Dynamics of RDX-Based Energetic Materials under CO2 Laser Heating. Combust Flame 1993;95:351–61.

[35] Wada Y, Hori K, Aria M. Combustion Mechanism of Mixtures of Guanidine Nitrate, Ammonium Nitrate, and Basic Copper Nitrate. Sci Technol Energ Mater 2010;71:83–7.

[36] Poole DR, Wilson MA. Composition and Process for Inflating a Safety Crash Bag. US Patent 4948439, 1990.

[37] Mendenhall IV., Taylor RD. Gas Generation with Copper Complexed Imidzole and Derivatives. US Patent 7470337 B2, 2008.

[38] Taylor RD, Mendenhall IV. Burn Rate Enhancement of Basic Copper Nitrate-Containing Gas Generant Compositions. US Patent 7998292 B2, 2011.

[39] Mendenhall IV., Smith RG, Taylor RD. Gas Generant Manufacture. US Patent 6436211 B1, 2002.

[40] Mendenhall IV., Taylor RD. Gas Generant Materials. US Patent 2006/0054257 A1, 2006.

[41] Mendenhall IV., Taylor RD. Substituted Basic Metal Nitrates in Gas Generation. US Patent 6958101 B2, 2005.

[42] Barnes MW, Mendenhall IV., Taylor RD. Ammonium Perchlorate-Containing Gas Generants. US Patent 7147733 B2, 2006.

[43] Yamato Y. Gas Generating Agent Composition and Gas Generator. US Patent 6517647 B1, 2003.

[44] Lund GK. Gas Generation via Elemental Carbon-Based Compositions. US Patent 8980023 B2, 2015.

[45] Barnes MW, Mendenhall IV. Chlorine-Containing Gas Generant Compositions Including a Copper-Containing Chlorine Scavenger. US Patent 2005/0016646 A1, 2005.

[46] Blomquist HR. Gas Generating Composition Comprising Guanylurea Dinitramide. US Patent 6117255, 2000.

[47] Mendenhall IV. Gas Generants Containing a Transition Metal Complex of Ethylenediamine 5,5'-Bitetrazole. US Patent 6689237 B1, 2004.

[48] Zeuner S, Hofmann A, Schropp R, Rodig K-H. Azide-Free Gas-Producing Composition. US Patent 6132537, 2000.

[49] Henry III GH, Solverson MS. Gas Generating Propellant. US Patent 5538567, 1996.

[50] McCave IN, Bryant RJ, Cook HF, Coughanowr CA. Evaluation of a Laser-

Diffraction-Size Analyzer for Use with Natural Sediments. J Sediment Res 1986;56:561–4.

[51] Demko AR, Allen TW, Thomas JC, Johnson M, Morrow GR, Reid DL, et al. Comparison of Commercially Available and Synthesized Titania Nano-Additives in Composite HTPB/AP Propellant. Propellants, Explos Pyrotech 2017;42:158–66.

[52] Resodyn. Resonant Acoustic® Mixing: Coating of Micron Materials With Nanopowder. n.d. http://resodynmixers.com/wp-content/uploads/2016/01/a13_b_nano_coat_micron_may09.pdf (accessed January 20, 2018).

[53] Resodyn. Resonant Acoustic ® Mixing: Blending Nano and Micron Sized Particles. n.d. http://resodynmixers.com/wp-content/uploads/2016/01/a08_a_nano_micro_powders_may09.pdf (accessed January 20, 2018).

[54] Vanarase A, Osorio J, Muzzio FJ, Coguill SL, Lucon P. Resonant Acoustic ® Mixing; Uniform Distribution of Minor Materials During Powder Mixing. JANNAF 36th Propellant Explos. Dev. Charact. Jt. Subcomm. Meet., 2010.

[55] Osorio JG, Muzzio FJ. Evaluation of Resonant Acoustic Mixing Performance. Powder Technol 2015;278:46–56.

[56] Hope KS, Lloyd HJ, Ward D, Michalchuk AAL, Pulham CR. Resonant Acoustic Mixing: Its Applications to Energetic Materials. New Trends Res. Energ. Mater., 2015, p. 134–43.

[57] Nellums RR, Terry BC, Tappan BC, Son SF, Groven LJ. Effect of Solids Loading on Resonant Mixed Al-Bi2O3 Nanothermite Powders. Propellants, Explos Pyrotech 2013;38:605–10.

[58] Carro RV. High Pressure Testing of Composite Solid Rocket Propellant: Burner Facility Characterization. MS Thesis, Dept. of Mechanical Material and Aerospace Engineering, University of Central Florida, Orlando, Florida, 2007.

[59] Carro R, Stephens M, Arvanetes J, Powell A, Petersen E, Smith C. High-Pressure Testing of Composite Solid Propellant Mixtures: Burner Facility Characterization. 41st AIAA/ASME/SAE/ASEE Jt Propuls Conf Exhib 2005:1–9.

[60] Robie R, Hemingway B, Fisher J. Thermodynamic Properties of Minerals and Related Substances at 298.15K and 1bar Pressure and at Higher Temperatures. US Geol Surv Bull 1978;1452.

[61] Kreitz KR, Petersen EL, Reid DL, Seal S. Relative Dispersion of Catalytic Nanoparticle Additives and AP Particles in Composite Solid Propellant and the Effect on Burnig Rate. AIAA, 2011, p. 1–8.

APPENDIX A

A-1: High pressure bolt used to hold propellant sample pellet

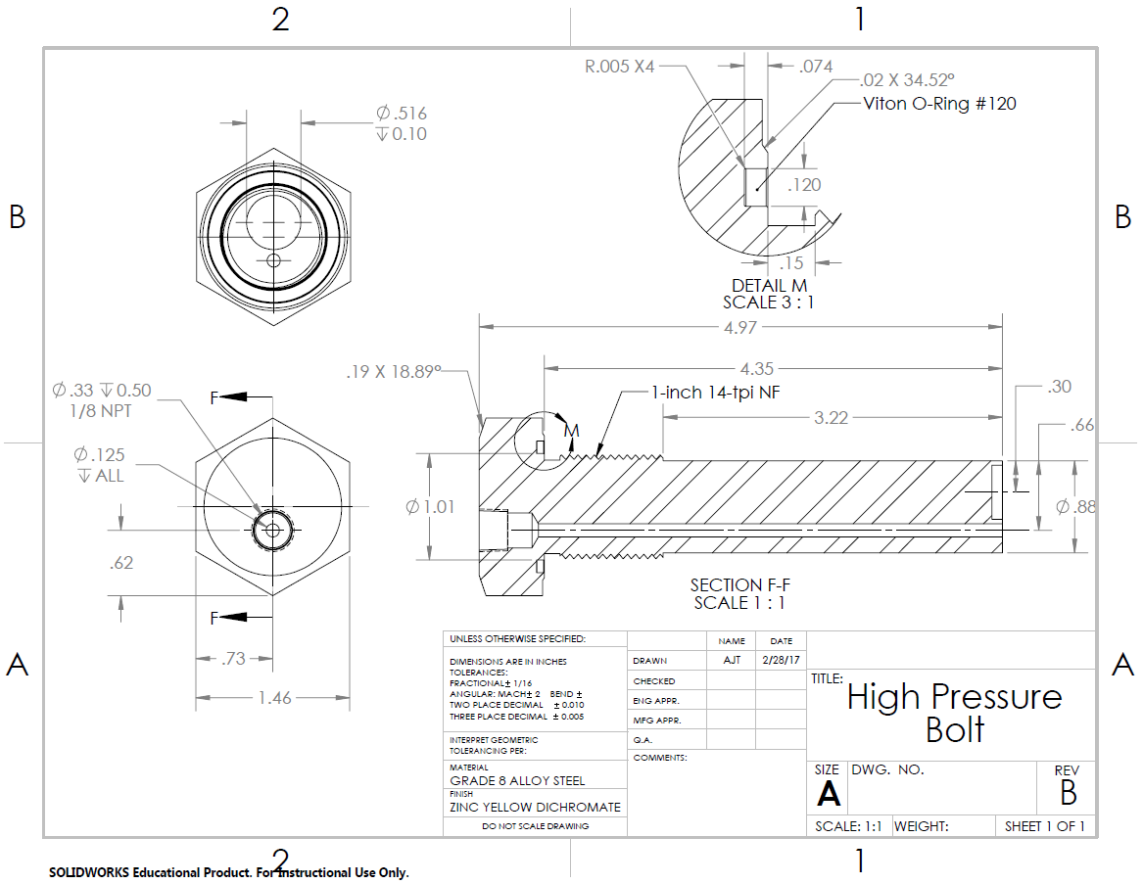

A-2: ProPEP calculation for baseline formulation

```
   Code                                  WEIGHT     D-H  DENS     COMPOSITION
      0 GUANIDINE NITRATE                53.360    -758  0.05190   6 H    1 C    4 N    3 O
      0 Basic Copper Nitrate             46.640    -867  0.12310   4 CU   6 H    2 N   12 O

THE PROPELLANT DENSITY IS  0.07107 LB/CU-IN OR   1.9673 GM/CC
THE TOTAL PROPELLANT WEIGHT IS  100.0000 GRAMS

NUMBER OF GRAM ATOMS OF EACH ELEMENT PRESENT IN INGREDIENTS

    3.205034 H
    0.437051 C
    1.942447 N
    2.476609 O
    0.388485 CU

****************************CHAMBER RESULTS FOLLOW    ****************************
  T(K)  T(F)  P(ATM)   P(PSI) ENTHALPY  ENTROPY   CP/CV    GAS   RT/V
  1898  2956    68.02  1000.00   -80.88   180.02  1.1930  3.011   22.588

SPECIFIC HEAT (MOLAR) OF GAS AND TOTAL =    11.257    10.892
NUMBER MOLS GAS AND CONDENSED =     3.011     0.384

 1.599804e+000 H2O         9.710727e-001 N2          4.342070e-001 CO2         3.799374e-001 Cu*
 4.234547e-003 Cu2O*       2.794185e-003 CO          2.461770e-003 H2          4.419452e-004 HO
 3.044616e-004 O2          2.562171e-004 NO          6.997382e-005 Cu          8.144705e-006 H
  1.07305E-06 O

THE MOLECULAR WEIGHT OF THE MIXTURE IS    29.449

****************************EXHAUST RESULTS FOLLOW    ****************************
  T(K)  T(F)  P(ATM)   P(PSI) ENTHALPY  ENTROPY   CP/CV    GAS   RT/V
   931  1216    1.00    14.70  -115.32   180.02  1.2371  3.011    0.332

SPECIFIC HEAT (MOLAR) OF GAS AND TOTAL =     9.459     9.242
NUMBER MOLS GAS AND CONDENSED =     3.011     0.367

 1.580852e+000 H2O         9.711952e-001 N2          4.369978e-001 CO2         3.450904e-001 Cu&
    0.0216924 Cu2O&          0.0216924 Cu2O&           0.0216924 Cu2O&

THE MOLECULAR WEIGHT OF THE MIXTURE IS    29.608

 **********PERFORMANCE:  FROZEN ON FIRST LINE, SHIFTING ON SECOND LINE**********

 IMPULSE   IS EX      T*      P*      C*    ISP*  OPT-EX  D-ISP      A*M   EX-T
   172.6  1.2119    1716   38.24  3457.6            8.67  339.6  0.10749    907
   173.1  1.1947    1729   38.47  3490.6   134.7    8.78  340.5  0.10852    931
```

A-3: ProPEP calculation for aluminum oxide formulations

```
   Code                                  WEIGHT     D-H  DENS     COMPOSITION
      0 GUANIDINE NITRATE                51.210    -758  0.05190   6 H    1 C    4 N    3 O
      0 Basic Copper Nitrate             44.790    -867  0.12310   4 CU   6 H    2 N   12 O
      0 ALUMINUM OXIDE                    4.000   -4000  0.06700   2 AL   3 O

THE PROPELLANT DENSITY IS  0.07091 LB/CU-IN OR   1.9628 GM/CC
THE TOTAL PROPELLANT WEIGHT IS  100.0000 GRAMS

NUMBER OF GRAM ATOMS OF EACH ELEMENT PRESENT IN INGREDIENTS

    3.076261 H
    0.419441 C
    1.864303 N
    2.495245 O
    0.078462 AL
    0.373076 CU

*****************************CHAMBER RESULTS FOLLOW   ******************************
  T(K)  T(F)  P(ATM)   P(PSI) ENTHALPY  ENTROPY   CP/CV    GAS   RT/V
  1841  2855    68.02  1000.00   -93.65   174.13  1.1863  2.890   23.537

SPECIFIC HEAT (MOLAR) OF GAS AND TOTAL =    11.191    11.088
NUMBER MOLS GAS AND CONDENSED =     2.890     0.408

 1.536134e+000 H2O        9.320462e-001 N2         4.174158e-001 CO2        3.654765e-001 Cu*
 3.921607e-002 Al2O3&     3.776879e-003 Cu2O*      1.971704e-003 CO         1.829446e-003 H2
 2.752822e-004 HO         1.834637e-004 O2         1.633923e-004 NO         3.668812e-005 Cu
  4.42814E-06 H

THE MOLECULAR WEIGHT OF THE MIXTURE IS    30.316

*****************************EXHAUST RESULTS FOLLOW   ******************************
  T(K)  T(F)  P(ATM)   P(PSI) ENTHALPY  ENTROPY   CP/CV    GAS   RT/V
   927  1209     1.00    14.70  -126.28   174.13  1.2271  2.890   0.346

SPECIFIC HEAT (MOLAR) OF GAS AND TOTAL =     9.467     9.397
NUMBER MOLS GAS AND CONDENSED =     2.890     0.412

 1.538096e+000 H2O        9.321280e-001 N2         4.193937e-001 CO2        3.718033e-001 Cu&
    0.0392161 Al2O3&        0.0392161 Al2O3&         0.0392161 Al2O3&

THE MOLECULAR WEIGHT OF THE MIXTURE IS    30.291

 **********PERFORMANCE:  FROZEN ON FIRST LINE, SHIFTING ON SECOND LINE**********

 IMPULSE   IS EX      T*      P*      C*    ISP*  OPT-EX  D-ISP      A*M   EX-T
   167.4  1.2037    1671   38.35  3345.6           8.80  328.5  0.10401    901
   168.5  1.1879    1683   38.56  3375.8   130.2   8.91  330.7  0.10495    927
```

A-4: ProPEP calculation for titania formulations

```
   Code                                  WEIGHT     D-H  DENS     COMPOSITION
      0 GUANIDINE NITRATE                51.210    -758  0.05190   6 H    1 C    4 N    3 O
      0 Basic Copper Nitrate             44.790    -867  0.12310   4 CU   6 H    2 N   12 O
      0 TITANIUM DIOXIDE                  4.000   -2551  0.15280   1 TI   2 O

THE PROPELLANT DENSITY IS  0.07264 LB/CU-IN OR   2.0105 GM/CC
THE TOTAL PROPELLANT WEIGHT IS  100.0000 GRAMS

NUMBER OF GRAM ATOMS OF EACH ELEMENT PRESENT IN INGREDIENTS

    3.076261 H
    0.419441 C
    1.864303 N
    2.477676 O
    0.050063 TI
    0.373076 CU

**************************CHAMBER RESULTS FOLLOW    ****************************
  T(K)  T(F)  P(ATM)    P(PSI) ENTHALPY  ENTROPY   CP/CV    GAS    RT/V
  1889  2941    68.02  1000.00   -87.85   174.80  1.1873  2.890   23.535

SPECIFIC HEAT (MOLAR) OF GAS AND TOTAL =    11.247    11.005
NUMBER MOLS GAS AND CONDENSED =     2.890     0.419

 1.535625e+000 H2O         9.320123e-001 N2          4.168261e-001 CO2         3.639888e-001 Cu*
 5.002558e-002 TiO2&       4.508315e-003 Cu2O*       2.563098e-003 CO          2.275507e-003 H2
 3.981140e-004 HO          2.729740e-004 O2          2.316113e-004 NO          6.146009e-005 Cu
   7.1909E-06 H

THE MOLECULAR WEIGHT OF THE MIXTURE IS    30.222

**************************EXHAUST RESULTS FOLLOW    ****************************
  T(K)  T(F)  P(ATM)    P(PSI) ENTHALPY  ENTROPY   CP/CV    GAS    RT/V
   950  1250    1.00    14.70  -121.29   174.80  1.2279  2.890   0.346

SPECIFIC HEAT (MOLAR) OF GAS AND TOTAL =     9.526     9.342
NUMBER MOLS GAS AND CONDENSED =     2.890     0.422

 1.538094e+000 H2O         9.321281e-001 N2          4.193953e-001 CO2         3.717970e-001 Cu&
 5.002559e-002 TiO2&       6.344783e-004 Cu2O&       7.856030e-006 H2          1.191400e-006 CO
 1.000000e-006 C           1.000000e-006 CH          1.000000e-006 CNH         1.000000e-006 CNHO
 1.000000e-006 CHO         1.000000e-006 CH2         1.000000e-006 CH2O        1.000000e-006 CH3
 1.000000e-006 CH4         1.000000e-006 CN          1.000000e-006 C2          1.000000e-006 C2H2
 1.000000e-006 C2H4        1.000000e-006 C2H4O       1.000000e-006 C2N2        1.000000e-006 C3
 1.000000e-006 C3O2        1.000000e-006 H           1.000000e-006 NH          1.000000e-006 HO
 1.000000e-006 NH2         1.000000e-006 H2O2        1.000000e-006 NH3         1.000000e-006 N2H4
 1.000000e-006 N           1.000000e-006 NO          1.000000e-006 NO2         1.000000e-006 N2O
 1.000000e-006 N2O3        1.000000e-006 N2O4        1.000000e-006 N2O5        1.000000e-006 O
 1.000000e-006 TiO         1.000000e-006 O2          1.000000e-006 TiO2        1.000000e-006 O3
 1.000000e-006 Ti          1.000000e-006 Cu          1.000000e-006 NHO         1.000000e-006 NHO2
 1.000000e-006 NHO2        1.000000e-006 NHO3        1.000000e-006 HO2         1.000000e-006 NO3
 1.000000e-006 N2H2        1.000000e-006 CN2         1.000000e-006 CN2         1.000000e-006 C2O
 1.000000e-006 CuO         1.000000e-006 Cu2         1.000000e-006 C2H         1.000000e-006 C2N
 1.000000e-006 CNO         1.000000e-006 N3          1.000000e-006 C&          1.000000e-006 TiC&
 1.000000e-006 TiC*        1.000000e-006 TiN&        1.000000e-006 TiN*        1.000000e-006 TiO&
 1.000000e-006 TiO*        1.000000e-006 TiO2&       1.000000e-006 TiO2*       1.000000e-006 Ti2O3&
 1.000000e-006 Ti2O3*      1.000000e-006 Ti3O5&      1.000000e-006 Ti&         1.000000e-006 Ti*
 1.000000e-006 N2O4&       1.000000e-006 N2O4*       1.000000e-006 Cu*         1.000000e-006 TiH2&
 1.000000e-006 N2H4*       1.000000e-006 CuH2O2&     1.000000e-006 CuO&        1.000000e-006 Cu2O*
 1.000000e-006 Ti&         1.000000e-006 TiO&        1.000000e-006 Ti3O5&      1.000000e-006 Ti3O5*
 1.000000e-006 CuCN&       1.000000e-006 Ti4O7&      1.000000e-006 Ti4O7*      1.000000e-006 H2O*

THE MOLECULAR WEIGHT OF THE MIXTURE IS    30.192

 **********PERFORMANCE:  FROZEN ON FIRST LINE, SHIFTING ON SECOND LINE**********

 IMPULSE   IS EX      T*      P*      C*    ISP*  OPT-EX  D-ISP      A*M    EX-T
   169.5  1.2046    1714   38.34  3388.3            8.79  340.7  0.10533     923
   170.6  1.1886    1726   38.55  3418.6   131.9    8.91  343.0  0.10628     950
```